Recent Advances of Logic Gate Circuits Based on Metallo-organic Compounds

Zhitao Qin,† Hongen Guo,† Xiaozhe Cheng, Zhitao Dou, Hong Lian,* Xifeng Li,* Wai-Yeung Wong, and Qingchen Dong*

ABSTRACT: With the rapid development of modern electronic technology, the demand for the fundamental electronic devices of logic gate circuits have been growing increasingly in the last decades. Metallo-organic compounds with unique chemical structures and optical and electronic properties are an important type of organic semiconducting materials for logic gate circuits. On the one hand, the excellent optoelectronic response characteristic of metallo-organic compounds allows them be able to achieve elementary logic functions. On the other hand, the structural diversity and adjustability of metallo-organic compounds could be utilized for simulating versatile high-speed, low-power logic operations by different types of stimuli. Up to now, various metallo-organic compounds such as metal complexes, organic-inorganic hybrid perovskites and MOFs materials have been explored and applied in logic gate circuits with attractive application potentials in fields of wearable electronics, sensors and artifical intelligence (AI), etc. In this review, we first introduce the basic concepts and classification of logic gate circuits, and then focus on analyzing the application principles and advantages of metallo-organic compounds including metal complexes, organic-inorganic hybrid perovskites and MOFs materials in logic gate circuits. Finally, we outline recent specific application cases of the above materials in logic gate circuits, demonstrating their potential in the design of high-performance logic gate circuits, and summarizes their challenges and future development trends. This review aims to provide a comprehensive overview of the research and application of metallo-organic compounds in the field of logic gate circuits.

1. Introduction

Logic gates, as the basic building blocks of digital electronic circuits, play a vital role in the fields of computer science, communication technology and digital electronics, etc. It is well known that traditional silicon-based materials have been widely used to manufacture logic gates and integrated circuits (IC). However, with the continuous progress and growing demands in the field of modern information technology (IT), silicon-based ICs have been encountering severe problems of physical limitation of miniaturization and heat dissipation. Therefore, researchers have begun to explore new materials and technologies to improve performance, reduce size and increase energy efficiency of logic gates to meet the needs of future advanced ICs.

Metallo-organic compounds (also known as organometallic compounds) are generally defined as metal complexes containing at least one metal-carbon (M-C) bond,[1] where metals may also be substituted by boron, silicon, phosphorus, and other elements. Metallo-organic compounds possess excellent physicochemical properties, including chemical stability, structural diversity, and unique photoelectrochemical properties. The first metallo-organic compound, $KPtCl_3(CH_2{=}CH_2)$ salt,[2] was synthesized by Zeise in 1827.[3] Throughout the history of metallo-organic compounds, this field of research has often been associated with the concept of free radicals. For example, organic compounds of alkali metals or other electropositive elements have long been used to generate persistent or active organic radicals through formal metal–carbon bond cleavage, which have been applied in electronics, materials, pharmaceuticals, and petrochemicals, etc.[4] Organic compounds, as the building blocks of organic semiconductor devices, play key roles in realizing electron transport and optoelectronic properties.[5] Devices based on metal-organic compound semiconductors have received extensive attention and research.[6] These devices combine the advantages of organic segments and metal elements, and they show enhanced extraordinary optoelectronic properties, which the individual component does not possess. The adjustability of their electronic structures and properties gives them broad application potential in electronic devices. In the research of logic gate circuits, the introduction of metallo-organic compounds provides a new way to achieve low power consumption, high performance, versatility and reconfigurability.[7-9] Optoelectronic devices based on small molecular metal complexes,[10,11] metal polymers,[12,13] organic-inorganic hybrid perovskites (OIHPs),[14,15] and metal-organic frameworks (MOFs)[16,17] have shown broad prospects and applications in logic circuits. These materials not only have the advantages of mechanical flexibility, high optical transparency, and easy fabrication, but also have tuneable optical and electrical properties that can achieve functions such as sensitive photoresponse and light modulation, which provide new options and possibilities for the design and optimization of logic circuits.

Logic gate circuit, that can implement Boolean logic operations, is the basis of modern electronic technology.[18] Logic gate circuits can be divided into elementary logic gates (such as NOT gates, AND gates, OR gates, *etc.*)[19,20] and composite logic gates (such as NAND gates, NOR gates, XOR gates, *etc.*).[21,22] They can achieve various complicated functions through different combinations. The research on logic gate circuits began in the early 20th century. Vacuum tubes were first used as switching elements.[23] Later, new materials and technologies such as transistors, ICs, and optoelectronic devices were developed. In recent several years, many research groups have made significant progress in the design, preparation, and practical application of metallo-organic compounds in logic gates.[24,25] These studies aim to push the frontier of logic gate

technology, improve the efficiency of computing and information processing, and open up new possibilities for the development of future electronic devices and systems.

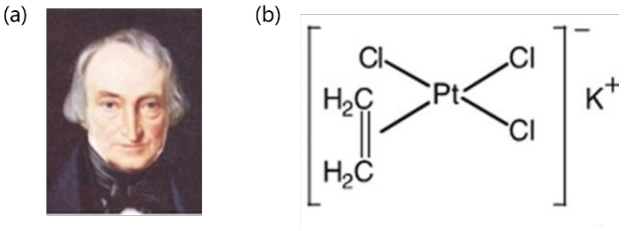

Figure 1. (a) W. C. Zeise (1789–1847). (b) The molecular structure of the first organometallic compound $KPtCl_3(CH_2{=}CH_2)$. Reproduced with permission from ref. 3. Copyright© 2019, WILEY-VCH.

Hence, with the rapid advancement of modern electronics, there is an increasing demand for new materials for logic gate applications. Undoubtedly, due to their unique structures and properties, metallo-organic compounds possess important potential in logic gate research and will continue to lead innovation in the field of electronic technology. This review briefly introduces the classification and functions of logic gate circuits, focusing on the application of metal complexes, OIHPs and MOFs materials in logic gate circuits. These metallo-organic compounds exhibit diverse structural features and excellent performance, enabling the design of high-speed, low-power and multifunctional logic gate circuits. Finally, the challenges and development of logic gate circuits based on metal-organic compounds are summarized, which might further inspire researchers to make breakthroughs in organic logic gate circuits and artificial intelligence (AI) in the future.

2. Concepts of Logic Gates

In the mid-19th century, mathematician George Boole introduced logical algebra, also known as Boolean algebra,[26] in his study of the laws of thought. Logic equations in Boolean algebra are often implemented using semiconductor devices. A truth table represents all possible combinations of input binary variables and their corresponding outputs in a logic system. Logical expressions in truth tables describe the relationship between system inputs and outputs. Logical algebra has become an important tool in the analysis and design of digital systems

A logic gate is a physical element used as the basic unit in digital circuits that performs logical operations on binary inputs and produces a single binary output. These gates typically use p-n diodes or metal-oxide-semiconductor field-effect transistors (MOSFETs) made of silicon, which are already widely used in commercial production.[27] Its types include resistor-diode logic,[28] direct-coupled transistor logic,[29] and four-layer device logic[30] with different characteristics. Complementary metal-oxide-semiconductors (CMOSs) based on MOSFETs technology have been identified as the fundamental technology for logic processing devices. In 1960, Mohamed M. Atalla and Dawon kang created CMOS technology using p-type and n-type transistors.[31] This low-power switching transistor paved the way for CMOS logic technology, which enables millions of logic gates to be packed into an integrated chip. Electronic circuits used to implement logical relationships are called gate circuits. At present, most of the commercial logic circuit components are metal oxides. With the development of new organic materials, organic semiconductor logic circuit components have gradually attracted people's attention. They have the low cost, printable, and bendable advantages and are expected to play an important role in the fields of flexible electronics, wearable devices, and photoelectric sensors.

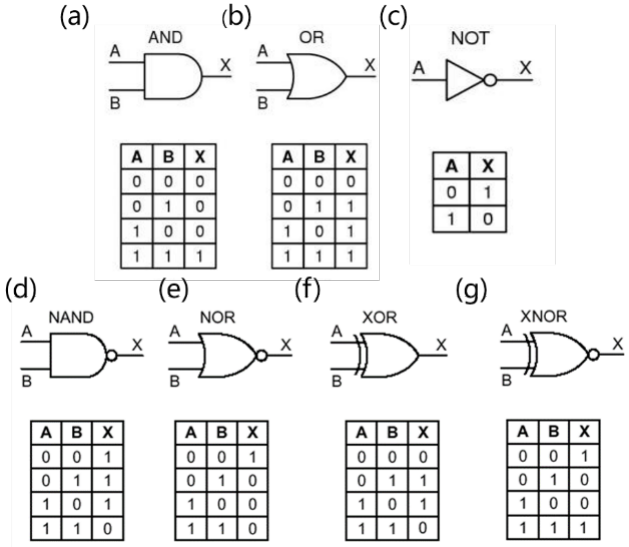

Figure 2. Seven common logic gate circuits. (a) AND gate. (b) OR gate. (c) NOT gate. (d) NAND gate. (e) NOR gate. (f) XOR gate. (g) XNOR gate.

As shown in Figure 2, logic gates include AND, OR, NOT, NAND, NOR, XOR, XNOR,[32] which can be divided into elementary logic gates and composite logic gates. These elementary gates can be combined to form composite logic circuits capable of performing various logical computing functions. In digital systems such as computers, different voltage levels are often used to indicate a logic "0" or logic "1" state. In a positive logic system, a high level represents a "1" and a low level represents a "0", while in a negative logic system, a high level represents a "0" and a low level represents a "1". Positive logic systems are the general convention unless otherwise stated. It should be noted that the high level and low level refer to voltage ranges rather than specific values. In addition, a logic "0" or logic "1" state can also be combined with an optical signal and photoelectric coordination signals to implement logical operations.[33]

2.1 Elementary Logic Gates

The AND, OR and NOT gates are the most elementary logic gate that can be used to perform AND, OR, and NOT operations, respectively.

2.1.1 AND gate

Figure 3a shows the two-input AND gate circuit. A and B are input logic variables and F is the output. D_1 and D_2 are diodes, U_{CC} is power source and R is for resistance. As long as one of the inputs A and B is low level, there must be a diode conducting to make the output F low level. The output of the AND gate takes high level only if all inputs are at the high level. In all other cases, the output is low level. When interpreted as a positive logic system, this means that the output of the AND gate is only a logic "1" if all inputs are in a logic "1" state. The AND operation, which is also called logic product, with two independent inputs A and B is written as $\boldsymbol{F=A\cdot B}$. Figure 3b and Figure 3c are the logical symbol and truth table of the AND gate.

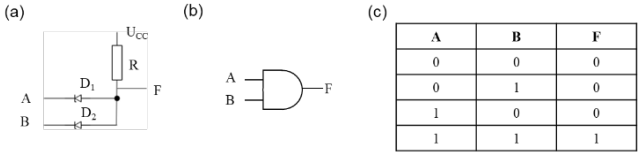

A	B	F
0	0	0
0	1	0
1	0	0
1	1	1

Figure 3. (a) Diodes AND gate circuits. (b) logic symbol of AND gate. (c) Truth table of AND gate.

2.1.2 OR gate

Figure 4a shows the two-input OR gate circuit. As long as one of inputs A and B takes high level, output F is at high level in a logic "1" state. Output F is in logic "0" state only if all inputs are at logic level of "0". The OR operation, which is also called logic addition, with two independent inputs A and B is written as $\boldsymbol{F=A+B}$. Figure 4b and Figure 4c are the logical symbol and truth table of the OR gate.

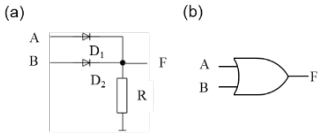

A	B	F
0	0	0
0	1	1
1	0	1
1	1	1

Figure 4. (a) Diodes OR gate circuits. (b) Logic symbol of OR gate. (c) Truth table of OR gate.

2.1.3 NOT gate

Figure 5a shows the one-input NOT gate circuit, which is also known as a "complementing circuit" or an "inverting circuit". The output is always the complement of the input, namely, a logic "0" at the input produces a logic "1" at the output, and vice versa. When the input A is at low level, the transistor is cut off, and the output F is high level. When input A is at high level, choose R_1 and R_2 reasonably, the transistor works in saturation state, and output F is low level. The NOT operation is written as $\boldsymbol{F=\overline{A}}$. Figure 5b and Figure 5c are the logical symbol and truth table of the NOT gate. Here, T is transistor.

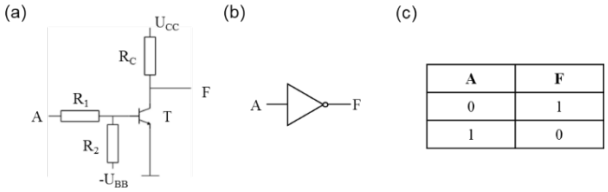

A	F
0	1
1	0

Figure 5. (a)Transistor NOT gate circuits. (b) Logic symbol of NOT gate. (c) Truth table of NOT gate.

2.2 Composite logic gates

In practical applications, AND gate, OR gate and NOT gate are usually combined in different ways to constitute various logical gate circuits and achieve composite logic operations. The common composite logic gate circuits are NAND, NOR, XOR, XNOR and AND-OR-INVERT gates.

2.2.1 NAND gate

Cascading a NOT gate at the output of the diode AND gate creates a NAND gate circuit. Figure 6a shows the truth table of a two-input NAND gate. As long as one of inputs A and B takes low level, the output F will be at high level; only when inputs A and B are at high level simultaneously, the output F is at low level. The NAND operation with two independent inputs A and B is written as $\boldsymbol{F=\overline{AB}}$. Figure 6b shows the logical symbol of NAND gate.

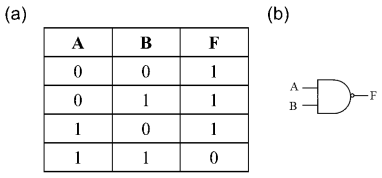

A	B	F
0	0	1
0	1	1
1	0	1
1	1	0

Figure 6. (a) Truth table of NAND gate. (b) Logic symbol of NAND gate.

2.2.2 NOR gate

Similarly, cascading a NOT gate at the output of the diode OR gate creates a NOR gate circuit. The truth table of a two-input NOR gate is shown in Figure 7a. As long as one of inputs A and B takes low level, the output F will be at high level; only when both inputs A and B take the high level, the output F will be at low level. The NOR operation with two independent inputs A and B is written as $\boldsymbol{F=\overline{A+B}}$. Figure 7b shows the logical symbol of the NOR gate.

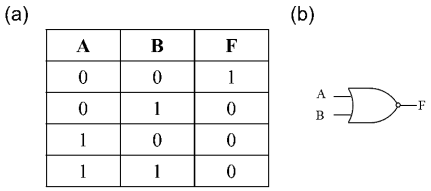

A	B	F
0	0	1
0	1	0
1	0	0
1	1	0

Figure 7. (a) Truth table of NOR gate. (b) Logic symbol of NOR gate.

2.2.3 XOR gate (Exclusive-OR)

The logical expression of XOR gate is $F=\bar{A}B+A\bar{B}$,also recorded as $F=A\oplus B$. The truth table for the XOR gate is shown in Figure 8a. When two variables take the same value, the result of the operation is 0; when two input variables take different values, the result of the operation is "1". If a XOR gate extends to multiple variables, when the number of "1" in the variables is even, the operation result is "0"; when the number of "1" in the variables is odd, the operation result is "1". The logical symbol of the XOR gate is shown in the Figure 8b.

(a)

A	B	F
0	0	0
0	1	1
1	0	1
1	1	0

(b)

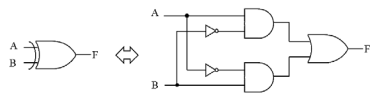

Figure 8. (a) True table of XOR. (b) Logic symbol of XOR.

2.2.4 XNOR gate (Exclusive-NOR gate)

The logical expression for the XNOR operation is $F=\bar{A}\bar{B}+AB=A\odot B$. Figure 9 shows the logical symbol of the XNOR gate, which is the complementary of the XOR gate, corresponding to the XOR gates followed by a NOT gate.

(a)

A	B	F
0	0	1
0	1	0
1	0	0
1	1	1

(b)

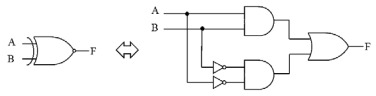

Figure 9. (a) True table of XNOR. (b) Logic symbol of XNOR.

2.2.5 AND-OR-INVERT gate

The AND-OR-INVERT gate circuit is equivalent to a combination of two AND gates, one OR gate and one NOT gate. Figure 10 shows the logical symbol for the four inputs AND-OR-INVERT gate, and the logical expression of which is $F=\overline{AB+CD}$.

(a)

A	B	C	D	F
0	0	0	0	1
0	0	0	1	1
0	0	1	0	1
0	0	1	1	0
0	1	0	0	1
0	1	0	1	1
0	1	1	0	1
0	1	1	1	0
1	0	0	0	1
1	0	0	1	1
1	0	1	0	1
1	0	1	1	0
1	1	0	0	0
1	1	0	1	0
1	1	1	0	0
1	1	1	1	0

(b)

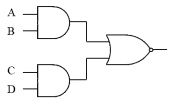

Figure 10. (a) True table of AND-OR-INVERT. (b) Logical symbol of the AND-OR-INVERT.

3. Logic gates application of metallo-organic compounds

Organic semiconducting materials are showing increasing promise in integrated circuits due to their rich structural diversity and solution processability.[34] As metal elements are introduced into the molecular backbone, some new properties and phenomena will appear. Therefore, as shown in Figure 11, metallo-organic compounds including small molecular metal complexes, metal-polymers, MOFs, and OIHPs exhibit mechanical flexibility, high optical transparency, ease of fabrication, and tuneable optical and electrical properties for sensitive photo response and light modulation, which have extensive application perspectives in novel logic circuits.[35]

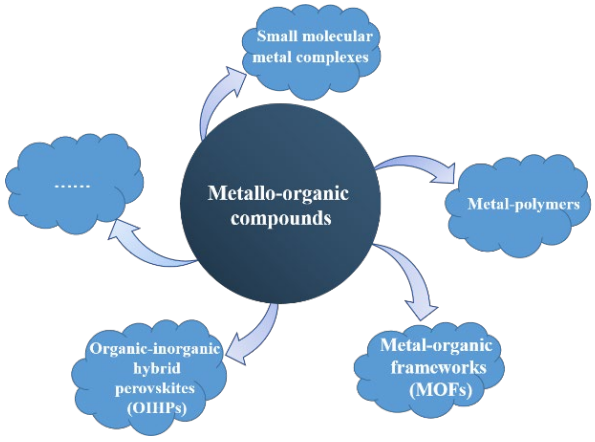

Figure 11. Simple classification of metallo-organic compounds.

Generally, optoelectronic devices that are capable of performing physicochemical changes as reaction to external stimulus can serve as switches or Boolean logic for fabrication of logic gate circuits in information processing and computing at the microelectronic or molecular level. To gain a profound insight into the working mechanism of organic logic gates, the current-voltage (I-V) or capacitance-voltage (C-V) curves should be first tested to understand their elctrical behaviors under either or both of the electrical and optical stimuli. The optical testing such as ultraviolet-visible spectroscopy (UV-Vis), fluorescence spectroscopy, and Raman spectroscopy is normally conducted to explore the optical properties of organic materials within circuits. Surface analysis techniques such as scanning electron microscopy (SEM) and atomic force microscopy (AFM) facilitate the observation of material microstructures, elucidating their impact on circuit performance. Dynamic testing yields crucial information on parameters like response time, power consumption, and stability of logic gate circuits. Furthermore, through computer simulation and modeling methods like density functional theory (DFT) and quantum chemical calculations, we can delve deeply into the electronic structure, energy level distribution, charge transport, carrier transport, and other physical processes of organic materials, offering vital theoretical and experimental support for optimizing and designing organic logic gate circuits. The following

describes the application of different types of metallo-organic compounds in logic gate circuits.

3.1 Logic gate applications of metal complexes

Metallo-organic compounds can be used to prepare resistance switching memories that implement multi-level storage and simple Boolean logic operations. In 2019, Zhang *et al.* synthesized a conjugated polymer PFTPA-Fc by introducing the redox-active moieties of triphenylamine (TPA) and ferrocene (Fc) onto the pendants of fluorene skeleton through Suzuki coupling polymerization and "Click" chemistry (Figure 12a). It can be seen clearly that the resultant polymer PFTPA-Fc exhibits triple oxidation behaviour and interesting memory-resistance switching properties in either the high resistance state (HRS) or low resistance state (LRS) due to the coexistence of TPA and Fc moieties(Figure 12b and c).[36] HRS currents monitored between 2 V show four distinguishable stages which are useful for the realization of multilevel memory, while LRS currents exhibit consecutive modulation and can be utilized in information processing applications. Then, authors analysed the resistive switching behaviour in detail and attempted to explore the simple Boolean logic operations for PFTPA-Fc based memristor device. As shown in Figure 12d, in the implementation of the Boolean logic OR gate, the authors defined the voltage applied to the top and bottom electrodes as input A and input B, respectively. The initial device current (10.36 μA) read at a specific voltage (0.2 V) is used as the criterion for distinguishing the output signal. If the device current at 0.2 V is higher than 10.36 μA after some operations, the output logic value is "1", otherwise the result is "0".

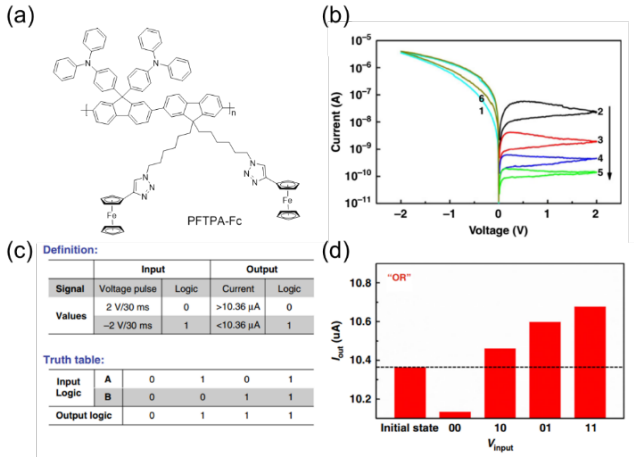

Figure 12. (a) Chemical structure of PFTPA-Fc. (b) Current–voltage curves of the ITO/PFTPA-Fc/Pt device; Realization of the OR logic gate function with PFTPA-Fc memristor. (c) Definition for the logic inputs/outputs and truth table. (d) Experimental results of the PFTPA-Fc device. Reproduced with permission from ref. 36. Copyright© 2019, Nature Publishing Group.

The truth table and experimental results of the above device current in response to different combinations of input pulses indicate that applying the input logic "1" to the top or bottom electrodes, or both, can change the device current to higher than 10.36 μA and gives the output logic "1". On the other hand, applying input logic "0" to both electrodes keeps the device current below 10.36 μA and results in output logic "0". This is very similar to the OR gate operation of the Boolean logic algorithm. Compared to the OR gate circuits in Figure 2, which require multiple components, this work achieves similar functionality on a single device with the simpler circuit structure, providing a feasible pathway for increasing IC density in the future.

The input signal for implementing a Boolean logic gate is not only limited to the electrical excitation signal, other external stimuli that can change the physical and/or chemical properties of the materials can also be used as input signals for logic gate applications. In 2017, Yang *et al.* designed and synthesized Eu^{3+}/Tb^{3+} cation-doped Cd-based long-afterglow coordination polymers (CPs), Eu-Cd-CPs, which exhibit tuneable excitation-dependent emission and tribochromic photoemission, and then obtained a new three-input, three-output optical logic gate based on the mechanism of the change in structural symmetry.[37] The design and achievement strategy of this logic gate is by defining time dependent, excitation-dependent and state-dependent luminescent properties as the input signals based on the long-afterglow and tribochromic photoemission, and normalized intensity values (the ratio of detected intensity to the maximum for each emission wavelength) at different wavelength as output signals O_1 (Output 1), O_2 (Output 2) and O_3 (Output 3), respectively. In this logic gate, the effective discrimination threshold is set as 30% of the maximum fluorescence intensity.

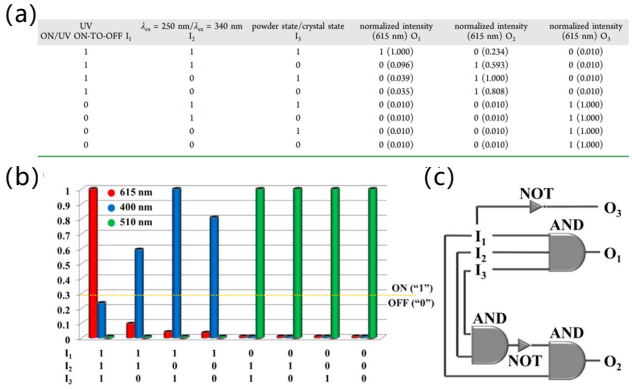

Figure 13. (a) Truth table for all of the possible strings of the three-input and three-output logic gate. (b) Normalized intensity outputs of Eu-Cd-CP at 615, 400, and 510 nm with eight various combinations obtained by the three crucial factors. Yellow dotted line represents the normalized intensity threshold value. (c) Three-input and three-output logic gate system for the Ln-Cd CPs. Reproduced with permission from ref. 37. Copyright© 2017, American Chemical Society.

When the normalized intensity is lower than 30%, the output signal is defined as OFF state "0". Otherwise, the result is "1". Figure 13a and Figure 13b show the truth table values of this logic gate which includes eight different combinations obtained by three crucial factors. Figure 13c shows the truth table values for output 1 forming an AND logic gate, the values of output 2 forming a NAND-AND logic gate, and the values of output 3 forming a NOT logic gate.

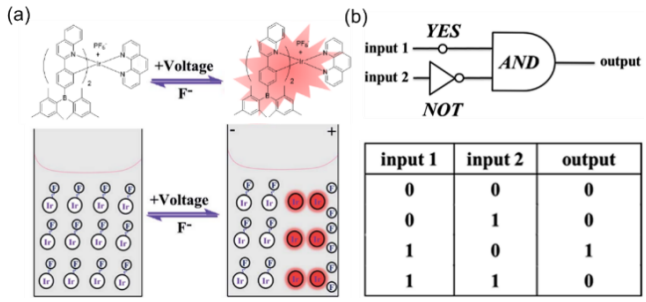

input 1	input 2	output
0	0	0
0	1	0
1	0	1
1	1	0

Figure 14. (a) Schematic diagram of the luminescent variation of complex $[(Bpq)_2Ir(Phen)]PF_6$ around the anode electrode triggered by fluoride and the electric field. (b) Schematic diagram of the formation and breakage processes of the B–F bond for complex$[(Bpq)_2Ir(Phen)]PF_6$ triggered by fluoride and the electric field and Logic circuit for a fundamental two-input, one-output INH. Reproduced with permission from ref. 38. Copyright© 2015, The Royal Society of Chemistry.

The fluorescence switching and spectral changes of metal complexes can also be utilized to realize different types of logic gate functions. In 2015, Lin *et al.* reported two phosphorescent Ir(III) complexes containing triarylboron moieties as shown in Figure 14a.[38] The phosphorescence of the complexes can be quenched by F^- through the formation of B-F bonds and restored through the rupture of B-F bonds under an electric field, therefore the phosphorescent switching can be achieved (Figure 14b). Based on this characteristic, authors proposed an inhibit (INH) logic gate with F^- and electric fields as the two inputs, and phosphorescence of the solution around the anode as the output signals. The corresponding truth table and the logic gate system for the INH function are shown in Figure14c. The INH gate was constructed by integration of NOT, YES and AND gates. This INH logic function takes logic state of "1" only when the phosphorescence of the solution around the anode is "quenched" in the presence of F^- ions (input 1) and in the absence of an electric field (input 2). Otherwise, phosphorescence can be observed in other cases.

The response of metallo-organic compounds to external stimuli is not limited to light and electric fields. The influence of chemical ions on their absorption spectra and fluorescence emission bands can also realize implement logic functions. In 2010, Liu et al. synthesized a square-planar Pt(II) terpyridyl complex which possesses three ordered intraligand charge transfer (ILCT), ligand-to-ligand charge transfer (LLCT), and metal to ligand charge transfer (MLCT) states, and the integrated logic functions were therefore achieved in a single molecular system (Figure 15a and b).[39] Herein, authors chose H^+, 1.0 equiv. of Fe^{3+} and Zn powder as three inputs I1, I2 and I3, respectively, while the molar extinction coefficient values of the absorption at 405 nm (MLCT as O1), 500 nm (ILCT as O2), 645 nm (LLCT as O3) and 850 nm (ligand-to-metal charge transfer (LMCT) as O4) were noted as outputs (the threshold values for O1 and O2 were set as 7.6×10^3 dm^3 mol^{-1} cm^{-1} and the threshold values for O3 and O4 were set as 3.5×10^2 dm^3 mol^{-1} cm^{-1}), to construct a three-input-four–output logic circuit.

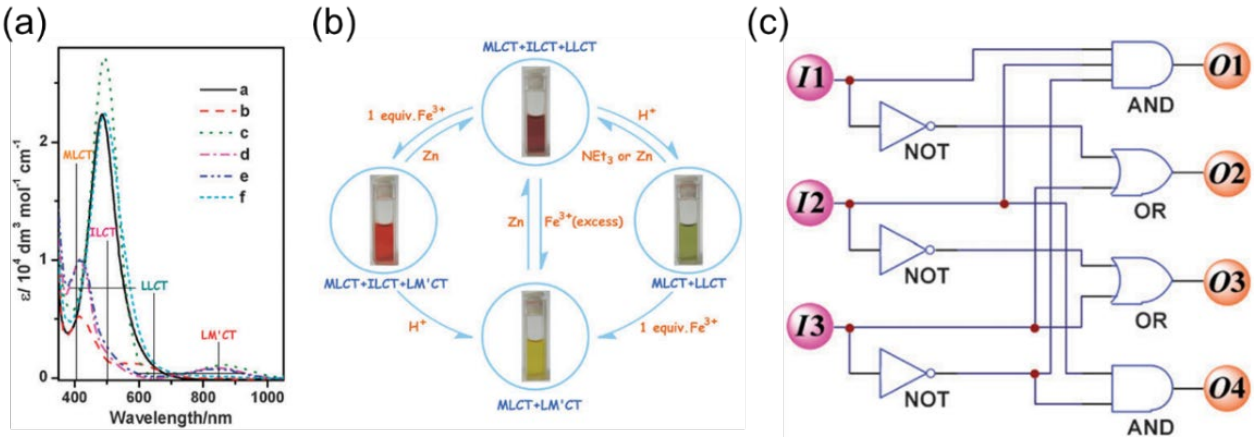

Figure 15. (a) UV–vis–NIR absorption spectra of a = 1, b = 1+HBF_4, c = 1+$Fe(ClO_4)_3$ (1.0 equiv.), d = 1+ HBF_4+$Fe(ClO_4)_3$ (1.0 equiv.), e = 1+$Fe(ClO_4)_3$ (excess), and f = 1+HBF_4 + $Fe(ClO_4)_3$ (1.0 equiv. or excess) + Zn in acetonitrile at room temperature. (b) the switching cycles associated with the four-state 1. (c) The combinational logic circuit. Reproduced with permission from ref. 39. Copyright© 2010, The Royal Society of Chemistry.

When the observed value is higher than the threshold value, it is set to signal "1" while a lower value produces signal "0". Thus, the molecular switch reads s string of three binary inputs and writes a specific combination of four binary outputs (Figure 15c). Truth table illustrates all the possible combinations of input data and the corresponding output string. The logic function equivalent to the truth table can be expressed as: **O1 = I1I2$\bar{I}$3 (AND), O2 = $\bar{I}$1 +I3 (OR), O3 = $\bar{I}$2 + I3 (OR), O4 = I2$\bar{I}$3 (AND)**. So the operations executed by the four-state molecular switch is equivalent to that of a combinational logic circuit integrating seven logic functions such as AND, OR and NOT. This work manifests that Pt(II) or other metal complexes can act as candidates for smart systems, which can integrate multiple switchable functions into a single molecule.

In 2017, Maurya *et al.* synthesized a novel 4-hydroxy-6-methyl-chromenone-based molecular receptor (**2a**), as shown in Figure 16a, which can selectively recognize Co^{2+} through a 2:1 binding mode between the ligand and Co^{2+} (2a-Co^{2+}complex) with the characteristic absorption peak

blue shifted from 344 nm to 332 nm, as shown in Figure 16b.[40] Due to the strong binding ability of CN^- to Co^{2+}, 2a-Co^{2+} complex can further coordinate with CN^- on the axial position, which results in two new peaks at 289 nm and 274 nm as well as the blue shift from 332 nm to 314 nm in the absorbance spectrum, and enhanced emission band at 431 nm. Then to fabricate an optical logic circuit, the Co^{2+} and CN^- are classified as two inputs in emission mode, a strong fluorescence intensity at 431 nm is considered as the "ON" state (output = 1), while a weak fluorescence intensity as "OFF" state (output = 0). 70% of the maximum fluorescence intensity of 2a (21000 a.u.) was taken as the threshold value. These results correspond to an IMPLICATION (IMP) logic gate and the working principle of the IMP logic gate is demonstrated in Figure16c.

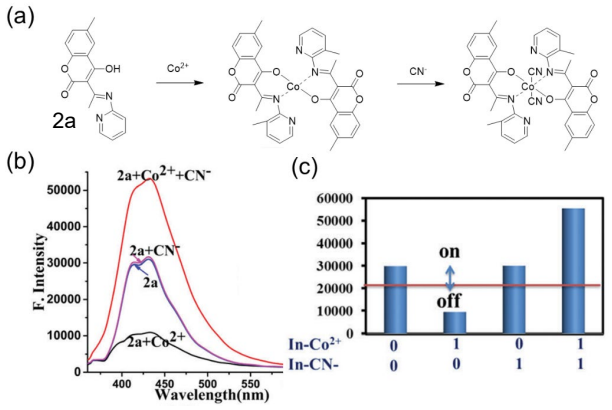

Figure 16. (a) Suggested sensing mechanism of 2a for Co^{2+} and the resulting complex for CN^- (b) Alteration in the emission spectra (c) The output intensities (bar chart) of 2a with Co^{2+} and CN^- as chemical inputs. Reproduced with permission from ref. 40. Copyright© 2017, The Royal Society of Chemistry.

The fluorescent switching properties of bimetallic terbium complexes can be used to achieve transfer and suppression logic functions. In 2015, Wang *et al*. synthesized a dimetallic terbium complex (L·Tb) with a new tripodal substituted-salicylic ligand (H_3L) and found that this carboxylate ligand is highly effective in the activation of Tb(III) emission, as shown in Figure 17a.[41] By taking L·Tb and $H_2PO_4^-$ as two chemical inputs, authors constructed a logic gate with TRANSFER and INH logic functions in the L·Tb-$H_2PO_4^-$ system. In the absence of two inputs, no fluorescence band in the range of 300-575 nm was observed (Figure 17b and c). Therefore, both output-1 and output-2 produce signals of "0" (entry 1). When L-Tb exists as input-1, three fluorescence bands appeared in the range of 300-575nm, which can be attributed to the ligand and Tb(III)-centred $^5D_4$ excited state to ^7F_J transitions with J = 6 and 5, respectively. Thus, output-1 and output-2 are both "1" (entry 2). When $H_2PO_4^-$ was introduced as input-2, no fluorescence bands were observed and both output-1 and output-2 become "0" (entry 3). However, in the presence of both inputs, the fluorescence band at 359 nm was observed but the two characteristic bands of Tb(III) ions at 495 and 550 nm were quenched, thus, output-1 produces signal of "1" and output-2 become "0". This is because that the "antenna" effect between the ligand and Tb(III) centre is suppressed due to the addition of phosphate anion, resulting in fluorescence bands turning "ON" to "OFF" significantly.

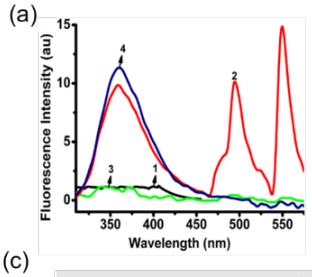

(c)

entry	input-1 L·Tb	input-2 $H_2PO_4^-$	output-1 359 nm	output-2 495/550 nm
1	0	0	0	0
2	1	0	1	1
3	0	1	0	0
4	1	1	1	0

Figure 17. (a) Logic gate system using L·Tb and phosphates as inputs and the intensity of the fluorescence emission at 359 or at 495 and 550 nm as the outputs. (a) Fluorescence spectra at different input states: (1) no inputs, (2) L·Tb, (3) $H_2PO_4^-$, and (4) L·Tb + $H_2PO_4^-$; (b) The combined logic circuit diagram; (c) truth table of logic gate. Reproduced with permission from ref. 41. Copyright© 2015, American Chemical Society.

In 2015, Mondal et al. reported the surface-confined heterometallic molecular triads (SURHMTs) (Os-PT/Cu/Ru-PT/Cu/Fe-PT) as fabricated on SiOx-based solid substrate by using optically rich and redox-active Fe^-, Os^-, and Ru-based terpyridyl complexes as metallo ligands and Cu^{2+} ions as linkers (Figure 18a).[42] Since Os^{2+}/Fe^{2+} centers and pyridyl moieties in the assembly can be oxidized and quaternized by NO^+ and then restore to initial spectrum by adding Et_3N and deionized water, therefore, a molecular-scale logic gate based on reversible optical property changes can be constructed. In order to develop such devices, three chemical inputs (NO^+ as input1, H_2O as input2, Et_3N as input3) and two optical outputs (absorbance at 577 nm and MLCT at 501 nm) were coded with Boolean logic functions, where the OFF and ON state are signal "0" and "1", respectively (Figure 18b). If monitoring the oxidation of centre in the assembly, time can be regarded as another input to construct more complex logic gates at the molecular scale with NO^+ as input1, time as input2, H_2O as input3, Et_3N as input4 and monitoring the emission intensity of the MLCT band at 501 nm as output. The truth table and four input-based logic circuit diagram (a combination of AND–NOR–AND gates) for this gate are exhibited in Fig 18c.

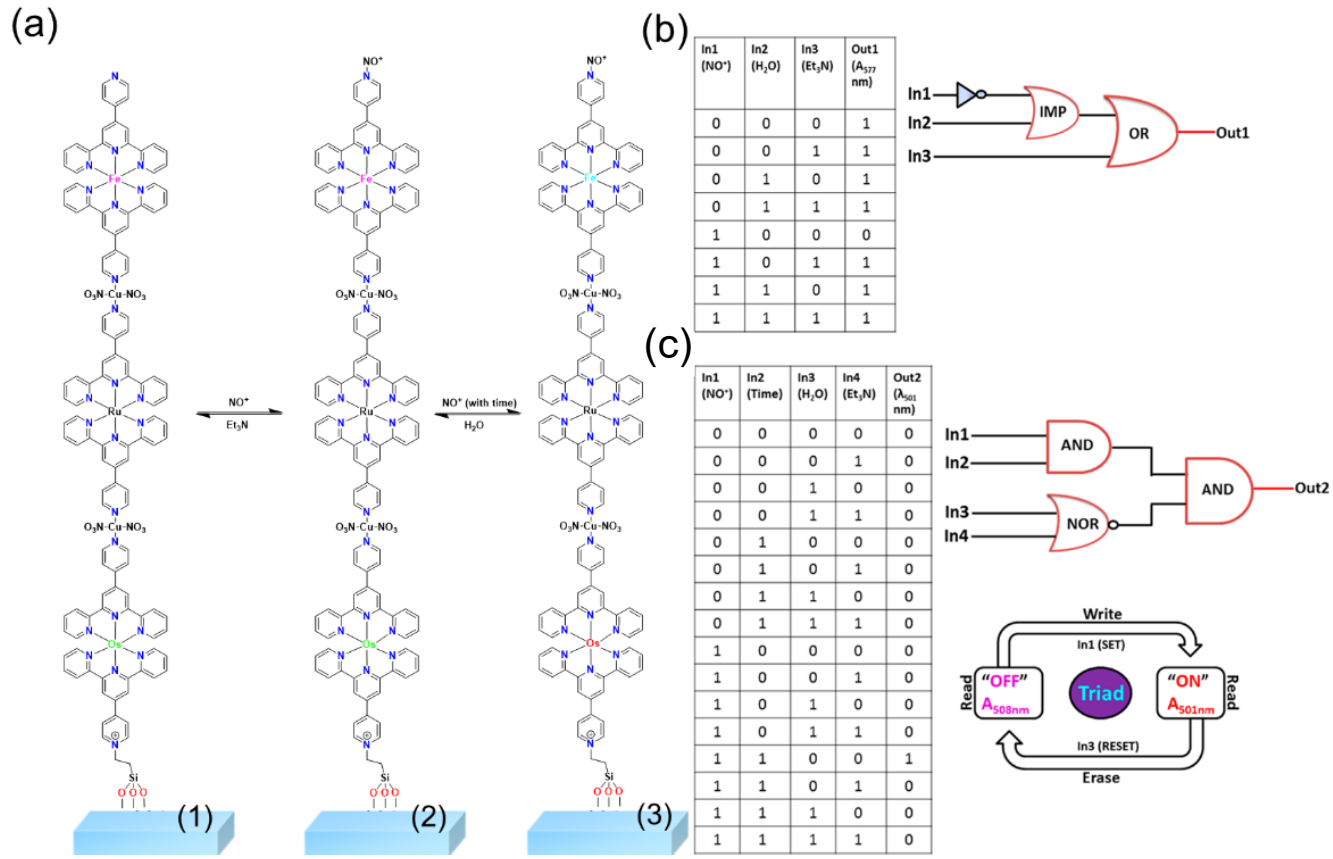

In1 (NO^+)	In2 (H_2O)	In3 (Et_3N)	Out1 (A_{577} nm)
0	0	0	1
0	0	1	1
0	1	0	1
0	1	1	1
1	0	0	0
1	0	1	1
1	1	0	1
1	1	1	1

In1 (NO^+)	In2 (Time)	In3 (H_2O)	In4 (Et_3N)	Out2 (A_{501} nm)
0	0	0	0	0
0	0	0	1	0
0	0	1	0	0
0	0	1	1	0
0	1	0	0	0
0	1	0	1	0
0	1	1	0	0
0	1	1	1	0
1	0	0	0	0
1	0	0	1	0
1	0	1	0	0
1	0	1	1	0
1	1	0	0	1
1	1	0	1	0
1	1	1	0	0
1	1	1	1	0

Figure 18. (a) Most plausible mechanism of oxidation/reduction and quaternization /dequaternization of Os-PT/Cu/Ru-PT/Cu/Fe-PT on glass substrates; neutral form of triad (1), quaternized form of triad upon reaction with NO^+ (2), and quaternized–oxidized form of the metal centers (Os^{3+}, Fe^{3+}) in the triad (3). (b) Truth table (left) and schematic (right) for a Boolean logic gate on the basis of the Os-PT/Cu/Ru-PT/Cu/Fe-PT heterotriads. The gate has NO^+, H2O, and Et_3N as inputs, namely, In1, In2, and In3, respectively, while absorbance at 577 nm serves as output (out1). (c) (left) Truth table for the heterotriad based logic gate with all possible variations according to 2n rule, where n=4. (right, upper) Reproduced with permission from ref. 42. Copyright© 2015, American Chemical Society.

By taking advantages of the multi-level redox process and near-infrared absorption signals of bimetallic complexes, ternary memories and logic circuits can be achieved. In 2015, Cui et al. designed and synthesized a diruthenium complex with a redox-active amine bridge, which shows three well-separated redox processes with exclusive near-infrared (NIR) absorbance at each redox state (Figure 19a and b).[43] Using NIR absorption signal as an output has the advantages of being low-energy, non-destructive, and low- interference with substrates. Through reductive electropolymerization of $3(PF6)_4$ on indium-tin-oxide (ITO) surface, poly-3^{n+} film was produced to further fabricate flip-flop and flip-flap-flop or ternary memory. Herein, three kind of flip-flop memories can be built from the poly-3^{n+} film by using any two redox states of poly-3^{3+} (In1 at 0.35 V), poly-3^{4+} (In2 at 0.75 V), poly-3^{5+} (In3 at 1.30 V) as inputs and their corresponding NIR absorbance wavelengths as outputs. For the flip-flap-flop or ternary memory, three electrochemical inputs (In1 at 0.35 V, In2 at 0.75 V, and In3 at 1.30 V) were first converted into three new input sequences (I1, I2, and I3) with three OR gates, then three cross-coupled NOR gates were followed to provide the memory and three optical outputs (Out1 at 750 nm, Out2 at 1170 nm, and Out3 at 1680 nm). Each output signal can display three levels of absorbance, which indeed mimics a truly ternary memory with the high, medium, and low absorbance of each output treated as the +1, 0, -1 level, respectively. The equivalent logic circuit of the device, truth table and corresponding logic memory operations are shown in the Figure 19c.

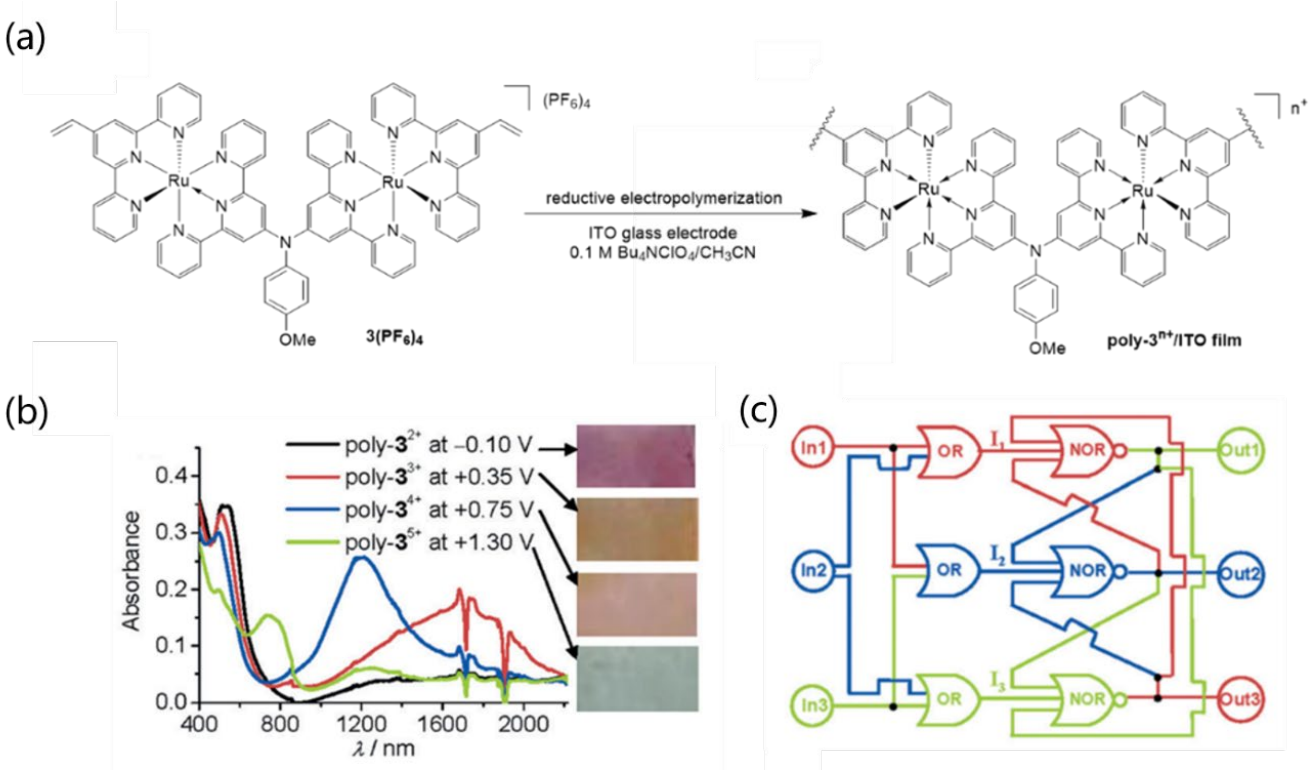

Figure 19. (a) Schematic representation for the reductive electropolymerization of $3(PF_6)_4$. (b) Absorption spectra and film picture of the poly-3^{n+}/ITO film at different redox states (Γ=5.0×10^{-9} mol cm^{-2}). (c) the flip-flap-flop or ternary memory based on the poly-3^{3+}/ITO film (Γ=1.4×10^{-9} mol cm$^{-2,}$ about 15–20 nm thick). Reproduced with permission from ref. 43. Copyright© 2015, WILEY-VCH.

3.2 Logic gate applications of organic-inorganic hybrid perovskites(OIHPs)

The crystal structure of OIHPs materials is usually ABX_3 type, where A is commonly an organic cation, B is a metal ion (usually Pb, Sn, *etc*.), and X is a halogen anion (such as Cl, Br, I, *etc*.). Organic cations are usually contained in the interstices of the perovskite structure and interact with the inorganic part through ionic or hydrogen bonds. Due to the excellent light absorption, long electron-hole diffusion length, ambipolar charge transport, unusual defect physics and tuneable band gap, OIHPs have been widely used in optoelectronics, such as solar cells, photodetectors, lasers, light-emitting diodes, transistors, *etc*. More recently, researchers reported the applications of perovskites for nonvolatile resistive switching random access memory (RRAM) and corresponding logic gate circuit. Benefiting from the excellent light response of OIHPs materials, In 2015, Lin *et al.* designed and prepared a light-sensitive logic gate device ITO/PEDOT:PSS/$CH_3NH_3PbI_3$/Cu with OR gate characteristics (the inputs A and B are the electric field and light illumination, respectively, and the output C is the current level).[44] Figure 20 shows the photo-induced logic OR device and its logical operation mechanism. In this logic gate device, due to the light-response induced two resistive states of perovskite material, authors employ the external electrical field and light illumination as input sources. The positive and negative electric fields are defined as the signal ‘‘0” and ‘‘1”, respectively, for input A; the light off and on states correspond to the signal “0” and “1”, respectively, for input B; the low and high current levels are defined as the signal “0” and “1”, respectively, for output C. The output is “0” (low current level) only when both inputs are signal “0”. The output signal is always “1” (high current level) if one or both of the inputs are signal “1”.

OIHP is also a type of photoelectric memory material that uses light to assist in low-voltage switching, storage and logic operations. In 2018, Zhou *et al.* also demonstrated an optoelectronic RRAM integrated with sensing and logic operations by adopting $CH_3NH_3PbI_{3-x}Cl_x$ as active layer. As shown in Figure 21a, this perovskite-based memory device exhibits low operation voltage of 0.1 V with the assistance of light illumination and can realize AND and OR logic gate functions.[45] Through the detailed spectral and energy level analysis, authors found that the photo-assisted low voltage switching is due to the large number of electron-hole pairs produced in perovskite under light illumination (Figure 21b and c). And these electron-hole pairs can be separated with a small bias of 0.1 V. The hole trap states at the perovskite/Au interface can capture photon-generated holes, shift the Fermi level of perovskite to the valence band, and lead to a lowered Schottky barrier. Meanwhile, more holes from the Au electrode can also be injected into the hole trap states in the perovskite, which further reduces the Schottky barrier and can form a quasi-ohmic contact between Au and perovskite corresponding to the low resistance state (LRS).

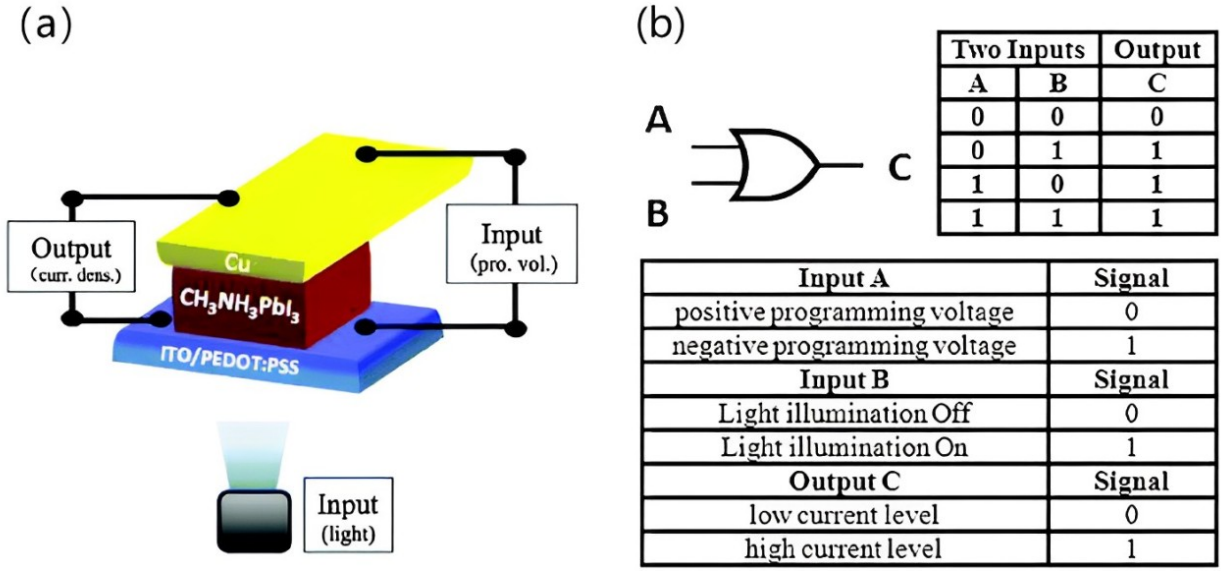

Two Inputs		Output
A	B	C
0	0	0
0	1	1
1	0	1
1	1	1

Input A	Signal
positive programming voltage	0
negative programming voltage	1
Input B	**Signal**
Light illumination Off	0
Light illumination On	1
Output C	**Signal**
low current level	0
high current level	1

Figure 20. Photo-induced logic OR device. (a) Schematic diagram of the light illumination induced logic OR gate. (b) State diagram of the logic OR device with two types of input sources and one output terminal. For the input source A, which is the electrical field, signals ''1'' and ''0'' represent the negative field and the positive field, respectively. For the input source B, which is the light illumination, signals ''0''and ''1'' represent light off and light on states, respectively. Reproduced with permission from ref. 44. Copyright© 2015, The Royal Society of Chemistry.

In the design of logic gates, for the inputs, the authors defined light pulse (> 3.2 mW cm^{-2}, 1 s) and electrical pulse (0.13 V, 100 μs) as logic "1", light pulse (<0.3 mW cm^{-2}, 1 s) and electrical pulse (0.01 V, 100 μs) as logic "0", respectively. For the outputs, HRS and LRS are defined as logic "1" and logic "0", respectively. Similarly, OR logic gates are implemented in a similar manner. The OIHP-based device not only achieves data storage but also offers application potentials in optical digital computation and optical quantum information.

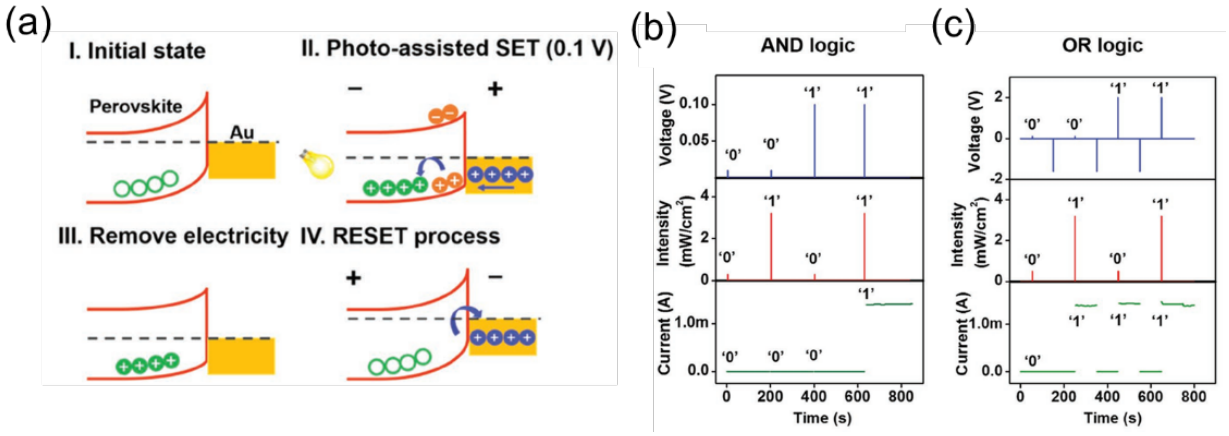

Figure 21. (a) Photo-assisted switching mechanism including four states: (I) initial state corresponding to HRS: hole trapping centers locate at the perovskite surface; (II) SET process: hole trap states are filled, shifting the Fermi level to the valence band; (III) remove light electricity: a lowered barrier and quasi ohmic contact are resulted corresponding to LRS; and (IV) electrical reset: holes are extracted from the trap states and a transition from LRS to HRS occurs. (b) A demonstration of AND logical operation. (c) A demonstration of OR logical operation. HRS and LRS are defined as logic "1" and logic "0" in both AND and OR logic operations. Reproduced with permission from ref. 45. Copyright© 2018, WILEY-VCH.

The bipolar spectral photo-responsive characteristics of OIHPs based self-powered photodetectors can also be used to realize high-speed, efficient, and multi-functional optoelectronic logic gate systems. In 2022, Woochul Kim *et al.* utilized the advantages of photodiodes such as large bandwidth and fast data transfer speed for construction of opto-electronic logic gates (OELGs).[46] They proposed a novel all-in-one OELG through employing the bipolar spectral photo-responsive characteristics of a self-powered perovskite photodetector (SPPD) with a back-to-back p^+-i-n-p-p^+ diode structure.

The SPPD consists of vertically stacked low-frequency-band perovskites ($FA_{0.5}MA_{0.5}Pb_{0.4}Sn_{0.6}I_3$, near infrared-Perov (NIR-Perov)) and high-frequency-band perovskites

($MAPbI_3$, visible-Perov (Vis-Perov)) (Figure 22a). It can be observed from the transmission electron microscopy (TEM) image that a PCBM layer was inserted as an n-type semiconductor between visible-calcite and NIR-calcite. Figure 22b illustrates the energy band diagram of the SPPD, which was investigated based on the UV photoelectron spectroscopy (UPS) results involving heavily doped p-type PEDOT:PSS,[47] Spiro-OMeTAD,[48] and n-type PCBM.[49] The Vis-Perov layer exhibits intrinsic (i-type) properties, while the NIR-Perov layer is slightly doped as p-type. Due to the low interfacial energy barrier, PCBM can transfer electrons into the Vis-Perov layer or the NIR-Perov layer at each heterojunction. The additional density of states (DOS) below the conducting band exists at the interface between the perovskite and PCBM layers, as calculated by density-functional theory (DFT). The bipolar spectral photoresponse is provided by a symmetric energy band structure consisting of two back-to-back p^+-i-n-p-p^+ perovskite diodes, a structure that critically supports charge transfer in both directions that can be responsive to irradiation conditions such as wavelength and power density.

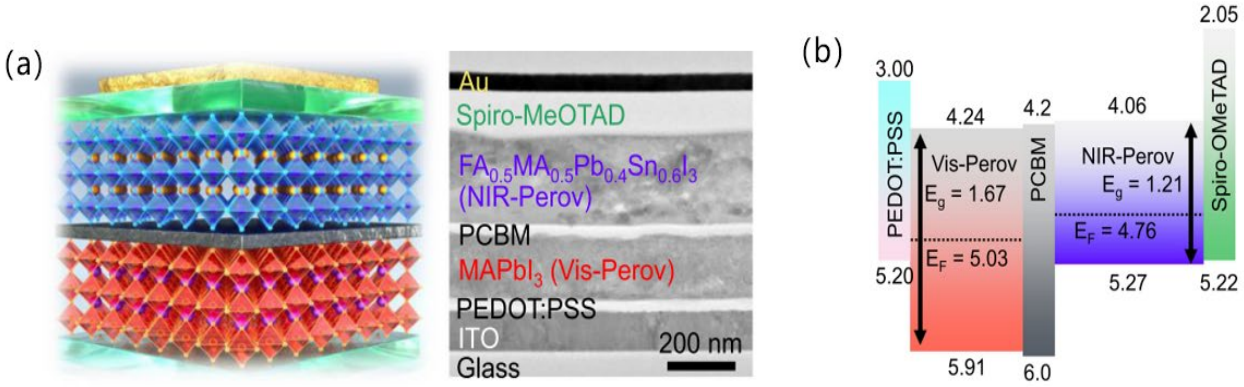

Figure 22. Characterization of the back-to-back SPPD. (a) Schematic of vertically stacked SPPD and its corresponding cross-sectional TEM image. (b) Energy band diagram of the p^+-i-n-p-p^+ structure. Reproduced with permission from ref. 46. Copyright© 2022 Nature Publishing Group.

Based on the bipolar spectral photoresponse of SPPDs, the researchers proposed a novel OELG system, which can perform five basic logic operations in the case of a single SPPD, i.e., "OR", "AND", "NAND", "NOR" and "NOT" (Figure 23a and b). The key element in the system is the "light gate modulator", and the core concept of which is to use light with different wavelengths and intensities as inputs. When two different wavelengths of light have similar photoconductance gains, fine-tuning the opposite photocurrent shift by light intensity modulation becomes a key strategy to realize the logic function. As an example, 625 nm light and 940 nm light are utilized for the next logic gate operation because their photoconductance gains (0.007 and 0.008, respectively) are well matched.

The polarity of the photocurrent of the SPPD can be adjusted by grating modulation. As shown in the Figure 23c, the output state of "1" or "0" is determined by the output positive or negative photocurrent, respectively. The output discrimination of the SPPD-OELG is based solely on the polarity of the photocurrent, not on the difference between the unipolar photoresponse and the reference level, which improves the accuracy and reliability of the logic gate device, and thus are independent of current variations or electrical noise. The OELG array platform with 64 SPPD pixels runs all five logic gates at 100% yield.

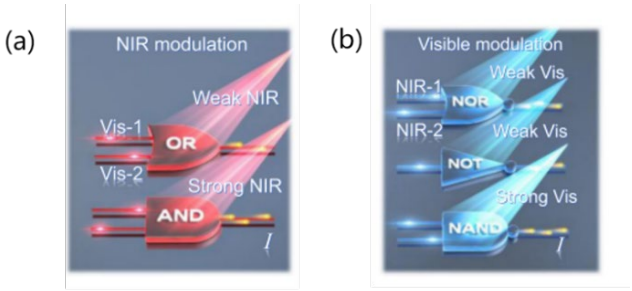

(c)

Input				Output		
Vis-1 (NIR-1)	Vis-2 (NIR-2)	OR	AND	NOR	NOT	NAND
0	0	0	0	1	1	1
1	0	1	0	0	0	1
0	1	1	0	0	-	1
1	1	1	1	0	-	0

Figure 23. Symbolic schematics of five OELGs executed with single SPPD. (a) "OR" and "AND" gates using two visible light inputs (625 nm) under NIR light (940 nm) gate modulations. (b) "NOR", "NOT", and "NAND" gates using NIR light inputs (940 nm) under visible light (625 nm) gate modulations. I is an output photocurrent. (c) Truth table of the five OELGs for the four input combinations. Reproduced with permission from ref. 46. Copyright© 2022, Nature Publishing Group.

3.3 Logic gate applications of metal–organic frameworks (MOFs)

The emergence of MOFs has been one of the most important events in chemistry and materials science over the past two decades. MOFs are multidimensional periodic reticular skeletons consisting of inorganic metal ions connected with organic ligands with controllable morphology, high specific surface area, abundant voids, and multifunctionality, and the MOFs materials can be self-assembled directly through the coordination of inorganic units with organic units. These organic units are usually multivalent organic carboxylates, which, when attached to metal units (e.g., Zn^{2+}, Co^{2+}, Cu^{2+}, Mg^{2+}, Ni^{2+}, Al^{3+}, *etc*.), can produce porous structures with well-defined pore size distributions and high specific surface areas.[50]

The unique advantages of MOFs with the activity of metal ions, flexible organic ligands that are functional groups with specific and excellent physical or chemical properties, as well as the presence of a regular three-dimensional spatial structure formed by the metal and organic ligands make MOFs highly versatile and controllable. Herein, MOFs, as a type of emerging multifunctional materials, have great potential in a number of important fields such as gas storage and separation, optical, electrical, and magnetic materials, chemical sensing, catalysis, and biomedicine, *etc*. Although most of the previously reported MOFs exhibit low conductivity or even insulating properties, a series of MOFs with semiconducting properties have still been successfully explored so far. The established semiconducting MOFs are mainly assembled by coordination reactions between transition metal ions (e.g., Fe, Co, Ni, Cu, *etc*.) and organic ligands with functional groups (e.g., $-NH_2$, -OH, and -SH).[51]

A logic gate based on a silicon circuit, whose output and input are electrical signals, can realize the logic operation of an electronic computer. Logic gates can convert input signals into specific output signals through Boolean logic operations. Recently, in addition to the application in the field of electronic computers, logic gates have also been used in the field of molecular computing, which breaks the limitations of traditional computers and can realize logic operations of various analytes in complex environment. Molecular logic gates are mainly composed of three parts: input-logic unit-output.[52-54] In general, most reaction processes are complex and require more precise mathematical models to describe the various nonlinear relationships among variables. The "threshold" introduced in the logic gate can distinguish between two different states in the reaction process. For example, different concentrations of analytes are used as input signals for fluorescence analysis, resulting in different fluorescence intensities as output signals. For the input signal, the presence or absence of input is defined as "1" and "0" respectively. If the resulting output intensity value is above or below the threshold, the logic gate will output "TRUE" (the true value of the Boolean logic operation is "1") and "FALSE" (the true value of the Boolean logic operation is "0"), respectively.

Especially, luminescent metal-organic frameworks (LMOFs) is a novel class of MOFs with luminescent properties, exhibiting both dye-doping capabilities and tuneable morphologies.[55] Their structures contain metal ions or ligands that have luminescent properties and are therefore capable of emitting visible or near-infrared light. LMOFs are often designed for applications of optical sensing, fluorescent labelling, photocatalysis, *etc*. Most logic gates based on LMOFs depends on the change of fluorescence intensity. The switch between "ON" and "OFF" of the logic gate can be controlled by different fluorescence quenching or enhancement effects (Figure 24a and b). LMOFs with π-conjugated structures or other aromatic ligands usually have strong fluorescence effects. Some guest species, such as quantum dots (QDs), organic dyes, and some metal compounds, can be encapsulated into LMOFs to generate luminescent effects. Using different fluorescent effects, "ON" and "OFF" states as well as different logic operations can be designed and achieved, such as AND, IMP,INH XOR, *etc*.[56,57]

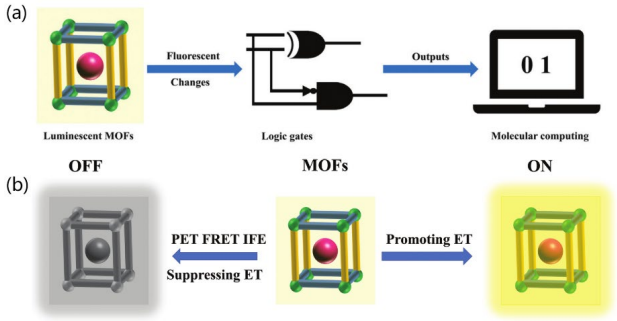

Figure 24. (a) Luminescent MOF as a molecular logic gate based on fluorescence changes. (b) Related mechanisms of quenching or enhancement effects of logic gates based on MOFs. Reproduced with permission from ref. 56. Copyright© 2015, The Royal Society of Chemistry.

In 2021, Zhang *et al*. constructed DNAzyme logic circuits for the analysis and imaging of multiple microRNAs in living cells using Cu/ZIF-8 nanoparticles (NPs) as nanocarriers for logic gate modules and Cu^{2+} cofactors for Cu^{2+}-dependent DNAzyme.[58] In this work, ZIF-8 NPs are utilized as a versatile vehicle to improve the intracellular performance of DNA logic circuits. The operations of Boolean logic are implemented using DNA molecules as input and output logic gate modules. The DNA logic circuits are designed based on the toehold-mediated strand displacement (TMSD) reaction, which allows for the conversion of a single nucleotide input signal into an output signal through chain migration and chain substitution reactions with logic gate modules. The TMSD reaction is entropy-driven and relies on the Watson-Crick base-pairing principle. The DNAzyme logic circuit mechanism proposed in this study is by utilizing the Cu^{2+}-dependent DNAzyme as the logic gate. Cu^{2+} is chosen as the effective cofactor for the Cu^{2+}-DNAzyme, and ZIF-8 NPs serve as nanocarriers for the delivery of the DNA logic gate elements into the cell. The Cu^{2+} ions are released from the ZIF-8 NPs, activating the Cu^{2+}-DNAzyme logic circuit. The logic gate modules are immobilized on the surface of the ZIF-8 NPs through electrostatic adsorption. The release of Cu^{2+} and the activation of the logic circuit are achieved through TMSD reaction. The DNA logic circuits implemented in this work

allow for the analysis and imaging of multiple microRNAs in living cells. The intracellular microRNAs, such as miRNA-155 and miRNA-21, serve as the biomolecular inputs, triggering the operation of "AND" and "OR" DNAzyme logic gates (Figure 25a and b). The logic gates are designed to respond to specific combinations of microRNAs, providing a means to detect and identify different microRNAs in complex cellular environments. The use of ZIF-8 NPs as a delivery vehicle for DNA logic gate modules addresses issues such as deficient delivery platforms, low delivery concentration, and degradability in complex biological environments.

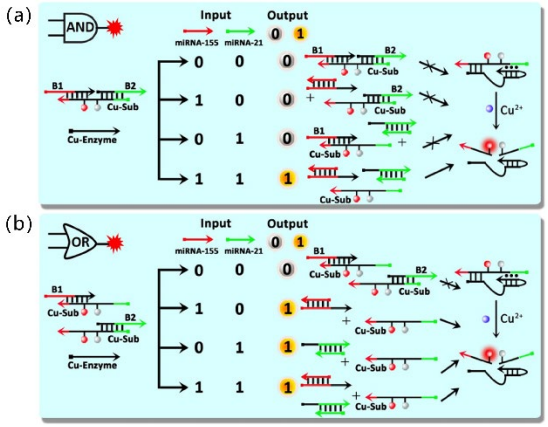

Figure 25. (a) "AND" schematic of a DNAzyme logic gate. (b) "OR" a schematic of a DNAzyme logic gate utilizing nanoscale Cu/ZIF-8 NPs to provide a logic gate module. Reproduced with permission from ref. 58. Copyright© 2021, American Chemical Society.

As mentioned above, LMOFs are a class of MOFs materials with fluorescent properties that can be combined with molecular logic gates to achieve high sensitivity, rapid response and intelligent recognition of biomolecules. In 2019, Dalapati *et al*. successfully synthesized a Hf^{IV}–based MOFs with hexanuclear UiO-66 topology by one-step solvothermal method using 3-methyl-4-phenylthieno[2,3-b] thiophene-2,5-dicarboxylic acid (H_2MPTDC) as a ligand.[59] Compared with conventional blue-emitting fluorescent materials, this blue-emitting MOFs material with wide energy bandgap exhibits higher efficiency and larger color gamut due to its adjustable 3D structure and π-conjugated backbone. It is known that, in addition to the intrinsic luminescent characteristic of metal ions and organic ligands, the optical properties of MOFs are also affected by weak Van der Waals interactions of MOFs with guest molecules through ligand bonding, π-π stacking or hydrogen bonding. Due to the reversible "on-off-on" switching properties of the fluorescence intensities of this MOFs material, it can be applied for the detection of Fe^{3+} and ascorbic acid (AA).[60] It was found that this Hf^{IV}–based MOFs exhibits high selectivity for Fe^{3+}, which is induced by the internal filtration effect (IFE). The MOF-Fe^{3+} system can be used for the selective fluorescence-triggered sensing of AA in aqueous media by eliminating the Fe^{3+} induced IFE. In the presence of AA, Fe^{3+} is reduced to Fe^{2+} by AA, which partially restores the initial blue fluorescence of MOFs. By utilizing different bioactive cations and small molecules (Fe^{3+}, AA, Fe^{2+}/H_2O_2) as inputs, the corresponding signal changes of the MOFs material as outputs, authors constructed a number of basic logic gates (e.g., NOT, YES, and OR), general-purpose logic gates (e.g., NAND and NOR), and multi-inputs logic gates to understand the complex fluorescence system.

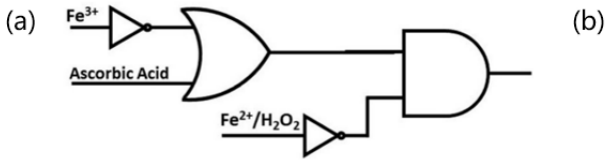

System	Input 1 (Fe^{3+})	Input 2 (Ascorbic Acid)	Input 3 (Fe^{2+}/H_2O_2)	Output (Emission Intensity)
1′	0	0	0	1 (high)
	1	0	0	0 (low)
	0	1	0	1 (high)
	0	0	1	0 (low)
	1	0	1	0 (low)
	0	1	1	0 (low)
	1	1	0	1 (high)
	1	1	1	0 (low)

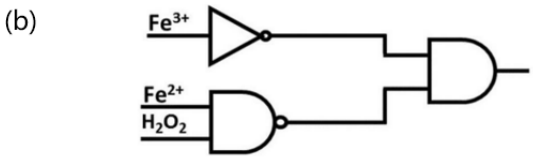

System	Input 1 (Fe^{3+})	Input 2 (Fe^{2+})	Input 3 (H_2O_2)	Output (Emission Intensity)
1′	0	0	0	1 (high)
	1	0	0	0 (low)
	0	1	0	1 (high)
	0	0	1	1 (high)
	1	0	1	0 (low)
	0	1	1	0 (low)
	1	1	0	0 (low)
	1	1	1	0 (low)

Figure 26. (a) Higher logic system built with the combination of NOT, OR and INH logic gates using a three-input system for fluorescent 1′. (b)Higher logic systembuilt with the combination of NOT, NAND and AND logic gates using a three-input system for fluorescent 1′. Reproduced with permission from ref. 59. Copyright© 2019, WILEY-VCH.

As shown in Figure 26a, Fe^{3+}, AA, Fe^{2+}/H_2O_2 are taken as three inputs, the corresponding fluorescence emission intensities act as outputs. Those exceeding the fluorescence intensity threshold are defined as the output "1", and those not exceeding the threshold are defined as the outputs "0". When Fe^{3+} or Fe^{2+}/H_2O_2 is present, the fluorescence is quenched, similar to an OR logic gate. In addition, AA treatment of the Fe^{3+} compound system restores fluorescence, forming a YES logic gate. In NOR logic operation, the output "1" is observed only when there is no input. The fluorescence is quenched under presence of Fe^{3+}, Fe^{2+}/H_2O_2, or both, which is in accordance with the NOR logic gate, as shown in Figure 26b. Similarly, NAND logic gates fluorescence is unaffected when there is no input or only one input, and quenches when both inputs are present. The research and logic gate design based on fluorescent

MOFs can be widely used in areas such as selective sensing of biomolecules and ions.

In the same year, Sun *et al*. designed a logic gate using lanthanide based LMOFs ($Eu_{0.059}Tb_{0.051}Gd_{0.8}$) system.[61] When excited with light of a specific wavelength, this LMOFs material is capable of emitting fluorescence at three different wavelengths (415 nm, 544 nm, and 616 nm). By introducing different ions as input and monitoring the fluorescence output, the authors demonstrate the ability to perform various Boolean logic operations. The NOR logic gate is first demonstrated (Figure 27a and b), which produces an output of 1 only when both inputs are 0. This is achieved by adding Fe^{3+} and VO_4^{3-} ions to this LMOFs solution. When Fe^{3+} is added alone, it quenches the emission at 616 nm, resulting in an output of 0. Likewise, when VO_4^{3-} is added alone, it quenches the emission at 415 nm, again resulting in an output of 0. However, when both Fe^{3+} and VO_4^{3-} are added together, the emission at both wavelengths is quenched.

XOR and INH logic gates can also be generated by introducing a third kind of ions as another input to the system (Figure 27c and d). The XOR gate produces an output of 1 when the input is 1/0 or 0/1 and an output of 0 when the input is 0/0 or 1/1. The INH gate produces an output of 1 on only one specific input (Figure 27e and f). These logic gates were realized by combining different combinations of Fe^{3+}, VO_4^{3-} and S^{2-} ions with the MOFs and analyzing the fluorescence output. In addition to individual logic gates, the researchers also demonstrated the ability to build complex logic circuits with multiple inputs and outputs. By combining different combinations of Fe^{3+}, VO_4^{3-} and S^{2-} ions with MOFs materials, the authors were able to generate multiple outputs from two or three inputs. This allows multiple analysis of different ions by using the same analyte input (Figure 27g and f).

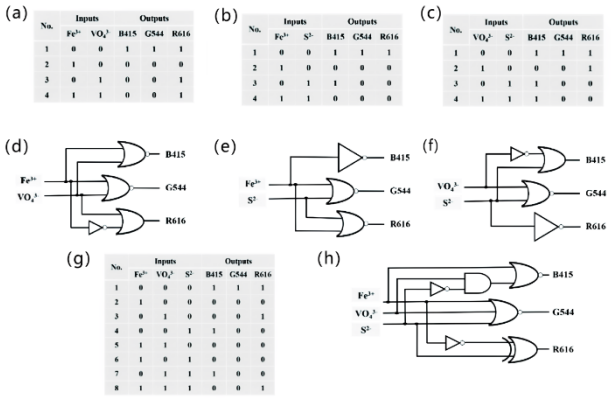

Figure 27. Truth tables of the double input Boolean logic gates (a) Fe^{3+} + VO_4^{3-}, (c) Fe^{3+} + S^{2-}, (e) VO_4^{3-} + S^{2-} and (g) Fe^{3+}, VO_4^{3-}, and S^{2-}. Electronic equivalent circuitries of the double input Boolean logic gates (b) Fe^{3+} + VO_4^{3-}, (e) Fe^{3+} + S^{2-}, (h) VO_4^{3-} + S^{2-} and(g) Fe^{3+}, VO_4^{3-}, and S^{2-}. Reproduced with permission from ref. 61. Copyright© 2019, The Royal Society of Chemistry.

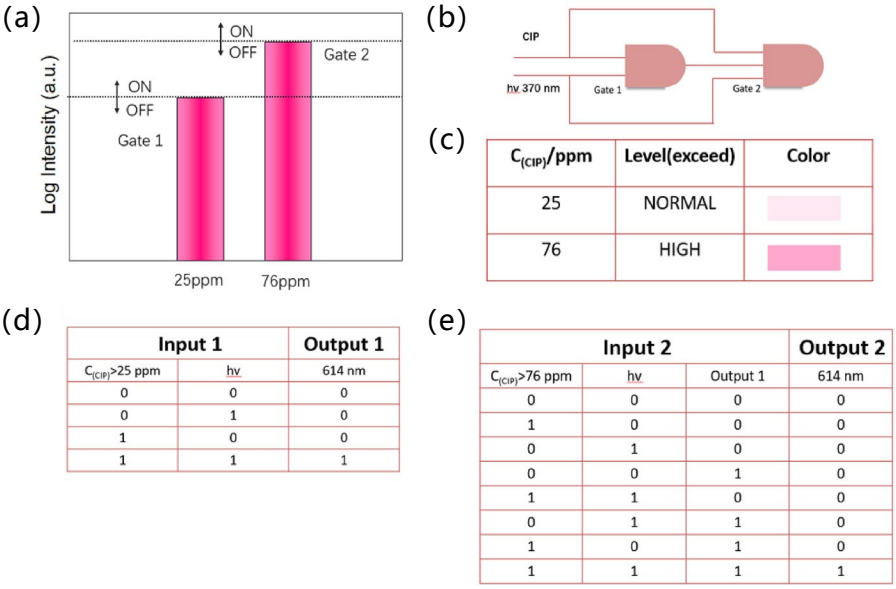

$C_{(CIP)}$/ppm	Level(exceed)	Color
25	NORMAL	
76	HIGH	

Input 1		Output 1
$C_{(CIP)}$>25 ppm	hv	614 nm
0	0	0
0	1	0
1	0	0
1	1	1

Input 2			Output 2
$C_{(CIP)}$>76 ppm	hv	Output 1	614 nm
0	0	0	0
1	0	0	0
0	1	0	0
0	0	1	0
1	1	0	0
0	1	1	0
1	0	1	0
1	1	1	1

Figure 28. (a) Column diagram of the normalized fluorescence intensities and the setting of threshold. (b) Specific circuitry of the logic gate operation. (c) Corresponding fluorescence, level for the concentrations of CIP. (d) Truth table of the 2-to-1 logic gate Gate 1. (e) Truth table of the 3-to-1 logic gate Gate 2. Reproduced with permission from ref. 62. Copyright© 2020, The Royal Society of Chemistry.

In 2020, Wang *et al*. designed and synthesized gallium-MOF (Ga-MOF1) as a turn-on fluorescent probe for the detection of ciprofloxacin (CIP) in urine.[62] They combine europium ions (Eu^{3+})-containing Ga-MOF1 hybrid with molecular logic gates for a real-time CIP concentration evaluation by intelligent discrimination. In the presence of CIP, the fluorescence intensity of the probe is selectively enhanced, allowing the detection of the compound in urine, as shown in Figure 28a. To further enhance the sensing capability, the researchers integrated two logic gates (Gate 1 and Gate 2) into the probe system to analyse the level of CIP in urine (Figure28b and c). Gate 1 is a two-to-one logic

gate that requires two inputs (CIP concentration and excitation wavelength) to be satisfied to generate an output signal. Gate 2 is a three-to-one logic gate that takes the output of gate 1 as an additional input. If all three inputs are satisfied, the series logic gate system will continue to operate and produce an output signal (Figure 28d and e). The "low", "normal" and "high" three different output states are defined based on the analysis of CIP levels in urine. The integration of logic gate operation with turn-on fluorescent probe can simplify the detection process without complex operations and expensive instruments. This probe system exhibits high sensitivity to CIP, which is not interfered by urine components and is suitable for practical applications.

Deviations from normal levels of singlet oxygen ($^1O_2$), hypochlorite ion (ClO^-), and copper ions (Cu^{2+}) in the human body may lead to severe health issues, such as lipid peroxidation,[63] arteriosclerosis,[64] and Alzheimer's disease.[65] Consequently, developing LMOFs logic circuit enables precise discrimination of these analytes in the clinical application, bearing considerable practical significance. In 2020, Gong and coworkers synthesized a whole-visible-spectra fluorescent nano-sized MOFs material (MOF-181) by incorporating three carboxyl-containing red-green-blue (RGB) dyes including TCPP (meso-tetra(4-carboxyphenyl) porphine), 5-AF (5-aminofluorescein) and DPA (5,5'-(anthracene-9,10-diyl) diisophthalicacid) into the core material MOF-181, as shown in Figure 29.[66] Employing chemical signals such as $^1O_2$, ClO^-, and Cu^{2+} as control inputs, the selective fluorescent response of DPA, 5-AF and TCPP acting as outputs, fundamental INH gates, complex half-adders, and multiple-input multiple-output (MIMO) logic circuits are successfully achieved on this platform (Figure 30a and b). The experimental results revealed that upon the generation of $^1O_2$, the intensity of the blue fluorescence channel diminishes, followed by a "domino" signal response in the green and red fluorescence channels due to fluorescence resonance energy transfer (FRET) effect, as displayed in Figure 30c. Similarly, in the presence of ClO^- or Cu^{2+}, the fluorescence signals of the RGB channels also alter due to the suppression of corresponding FRET effect. Based on this responsive mechanism, a novel MIMO logic circuit was designed by combining MOF-801-57 NPs and OR, INH, and NOR gates with appropriately set thresholds to achieve the desired logic operations. Notably, the fluorescence of these nanoscale MOFs is minimally influenced by various cations, anions, and amino acids within the human body, underscoring their reliability for applications in biomedicine. Figure 30d shows the truth table of a compound logic circuit with three-inputs and three-outputs.

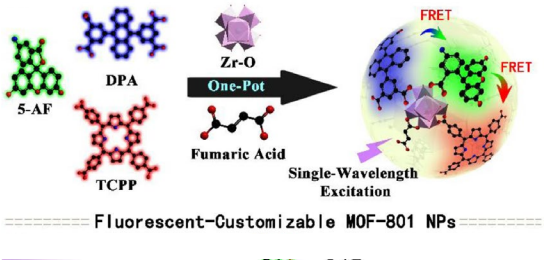

Figure 29. Schematic illustration for the synthesis of dyes-doped MOF-801 NPs using an in situ one-pot synthetic strategy. Fumaric acid acts as the ligand of MOF-801, and three functional dyes (DPA, 5-AF and TCPP) serve as the co-modulators to form the framework. Reproduced with permission from ref. 66. Copyright© 2020, The Royal Society of Chemistry.

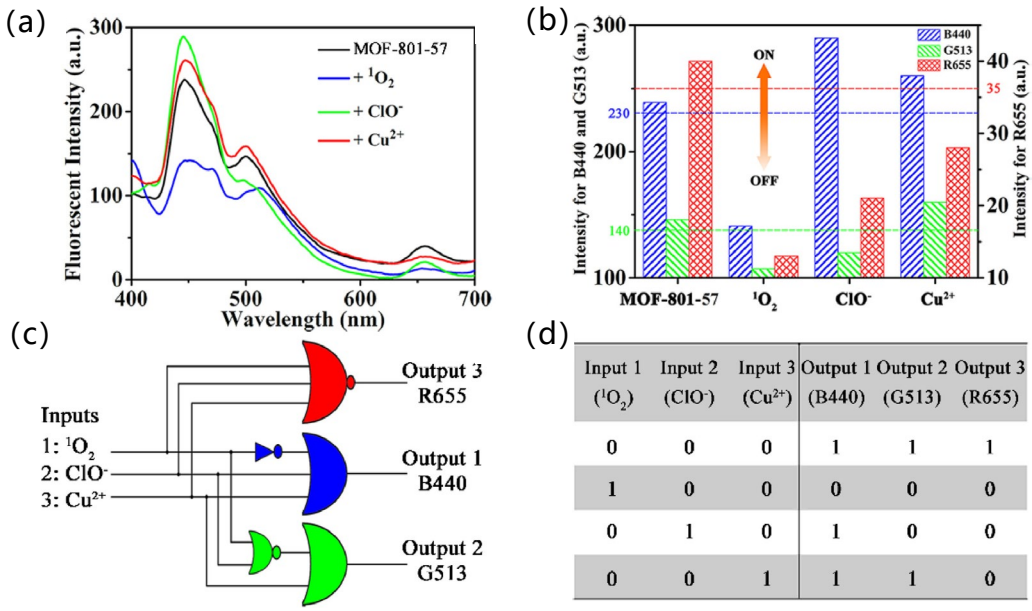

Input 1 ($^1O_2$)	Input 2 (ClO^-)	Input 3 (Cu^{2+})	Output 1 (B440)	Output 2 (G513)	Output 3 (R655)
0	0	0	1	1	1
1	0	0	0	0	0
0	1	0	1	0	0
0	0	1	1	1	0

Figure 30. (a) Fluorescent spectra of MOF-801–57 NPs (50 μg mL^{-1}) before and after the separate treatment of $^1O_2$, ClO^- and Cu^{2+} in HEPES buffer solution. (b) Column diagram of the fluorescent intensities at B440, G513 and R655 towards different signals: $^1O_2$, ClO^- and Cu^{2+}, and the dashed lines show the thresholds (B440:230; G513:140; and R655:35) of the Boolean logic gates. (c) Logic representation and (d) the truth table of a compound logic circuit with three-input and three-output fluorescence. Reproduced with permission from ref. 66. Copyright© 2020, The Royal Society of Chemistry.

4. Conclusions and Perspectives

To conclude, this review summarized the development of metallo-organic compounds such as small molecular metal complexes, OIHPs and MOFs materials in logic gate circuits in recent years, focusing on the working principles of basic and complex Boolean logic operations. Unlike the traditional silicon-based circuits whose output and input are only electrical signals, metallo-organic compounds-based logic gates can use light, electrical and chemical stimuli as inputs to implement complex logic circuits. In addition to the application in the field of optoelectronic devices, metallo-organic compounds-based logic gates have also been used in the field of molecular computing. It holds great prospective to break the limitations of traditional computers encountered and can realize smart and composite logic operations in complex environments. Different metal-organic materials with different device architectures have enabled significant advances in logic gates, eventually leading to innovations in multifunctional and integrated circuits. However, there are still several challenges need to be addressed and overcome to further exploit high performance metallo-organic logic gates and propel the industrialization of them for practical application.

Based on the research and investigation in the references, we outline several future challenges and directions in metallo-organic logic gates, providing some suggestions to researchers working in related disciplines. (1) The electronic interaction between the metal centre and organic framework has an important impact on the photoelectric properties of the material, but the intrinsic mechanism of some of them is still unclear and requires further research and exploration. This will help us rationally design materials with specific optoelectronic properties for pre-defined logic gate circuits. (2) Many metallo-organic compounds are prone to undergo decomposition or degradation under high temperature, high humidity or long-term use, thus affecting the reliability and lifetime of their electronic devices. In addition, there are also some constraints of metal-organic materials, such as the purity of the material, the uniformity of the film, and the difficulty of large-area preparation. Therefore, the further develop of new metallo-organic compounds with better solubility and new manufacturing techniques is necessary to improve the quality of films and device performance based on metallo-organic compounds. (3) Although metallo-organic compounds exhibit superior structure adjustability and flexibility, their electron mobility and conductivity are still low as compared to silicon and metal oxides, which need to be boosted to allow them suitable for application in high-performance electronic devices. (4) *In-situ* structure and property characterization techniques should be explored and conducted to disclose the working mechnism of metallo-organic logic gates under electrical and optical stimuli, especially for those with non-volatile memory characteristics.

Overall, metallo-organic compounds are expected to become an important component of next-generation logic devices in the future. Further research on logic gate circuits based on metallo-organic compounds is likely to achieve major breakthroughs and open up innovative prospects for applications in green electronics, degradable devices, flexible biosensors, and neuromorphic computing, *etc*.

AUTHOR INFORMATION

Corresponding Author

Hong Lian—*MOE Key Laboratory of Advanced Display and System Applications, Shanghai University, 149 Yanchang Road, Jingan District, Shanghai 200072, China. School of Mechanical & Electronic Engineering and Automation, Shanghai University, 99 Shangda Road, Baoshan District, Shanghai 200444, China.* Email:honglian@shu.edu.cn.

Xifeng Li—*MOE Key Laboratory of Advanced Display and System Applications, Shanghai University, 149 Yanchang Road, Jingan District, Shanghai 200072, China. School of Mechanical & Electronic Engineering and Automation, Shanghai University, 99 Shangda Road, Baoshan District, Shanghai 200444, China.* E-mail: lixifeng@shu.edu.cn

Qingchen Dong—*MOE Key Laboratory of Advanced Display and System Applications, Shanghai University, 149 Yanchang Road, Jingan District, Shanghai 200072, China. School of Mechanical & Electronic Engineering and Automation, Shanghai University, 99 Shangda Road, Baoshan District, Shanghai 200444, China.* E-mail: qcdong@shu.edu.cn.

Author

Zhitao Qin—*School of Mechanical & Electronic Engineering and Automation, Shanghai University, 99 Shangda Road, Baoshan District, Shanghai 200444, China*.

Hongen Guo—*MOE Key Laboratory of Advanced Display and System Applications, Shanghai University, 149 Yanchang Road, Jingan District, Shanghai 200072, China. School of Mechanical & Electronic Engineering and Automation, Shanghai University, 99 Shangda Road, Baoshan District, Shanghai 200444, China. School of Mechanical & Electronic Engineering and Automation, Shanghai University, 99 Shangda Road, Baoshan District, Shanghai 200444, China.*

Xiaozhe Cheng—*MOE Key Laboratory of Interface Science and Engineering in Advanced Materials, Taiyuan University of Technology, 79 Yingze West Street, Taiyuan, 030024, China. School of Mechanical & Electronic Engineering and Automation, Shanghai University, 99 Shangda Road, Baoshan District, Shanghai 200444, China.*

Zhitao Dou—*School of Microelectronics, Shanghai University, Shanghai 201800, China.*

Wai-Yeung Wong—*Department of Applied Biology and Chemical Technology, The Hong Kong Polytechnic University (PolyU), Hung Hom, Hong Kong, China*.

Author Contributions

† These people contribute equally to this work.

Notes

The authors declare no competing financial interest.

ACKNOWLEDGMENT

This work was supported by the financial support from the National Natural Science Foundation of China (Grant No.: 62174116 and 61774109) and the start-up fund from Shanghai University. W.-Y. W. thanks the financial support from the Hong Kong Research Grants Council (PolyU 15307321) and Ms Clarea Au for the Endowed Professorship in Energy (847S).

REFERENCES

(1) Patra, M.; Gasser, G. Organometallic compounds: an opportunity for chemical biology? *ChemBioChem.* **2012,** *13*, 1232-1252.

(2) Zeise, W. C. Von der Wirkung zwischen Platinchlorid und Alkohol, und von den dabei entstehenden neuen Substanzen. *Ann. Phys.* **1831,** *97*, 497-541.

(3) Wentrup, C. Zeise, Liebig, Jensen, Hückel, Dewar, and the Olefin π-Complex Bonds. *Angew. Chem. Int. Ed.* **2020,** *59*, 8332-8342.

(4) Kaim, W. Sites of Electron Transfer Reactivity in Organometallic Compounds. *Eur. J. Inorg. Chem.* **2020,** 875-878.

(5) Chan, N. H.; Gair, J. J.; Roy, M.; Qiu, Y.; Wang, D.-S.; Durak, L. J.; Chen, L.; Filatov, A. S.; Lewis, J. C. Insight into the Scope and Mechanism for Transmetalation of Hydrocarbyl Ligands on Complexes Relevant to C–H Activation. *Organometallics* **2020,** *40*, 6-10.

(6) Quintana-Romero, O. J.; Ariza-Castolo, A. Complex molecular logic gates from simple molecules. *RSC Adv.* **2021,** *11*, 20933-20943.

(7) Shan, Z.; Hu, X.; Wang, X.; Tan, Q.; Yang, X.; Li, Y.; Liu, H.; Wang, X.; Huang, W.; Zhu, X. Phonon-Assisted Electro-Optical Switches and Logic Gates Based on Semiconductor Nanostructures. *Adv. Mater.* **2019,** *31*, 1901263.

(8) Tybrandt, K.; Forchheimer, R.; Berggren, M. Logic gates based on ion transistors. *Nat. Commun.* **2012,** *3*, 871.

(9) Sordan, R.; Traversi, F.; Russo, V. Logic gates with a single graphene transistor. *Appl. Phys.* **2009***, 94*, 073305.

(10) Ma, D.-L.; He, H.-Z.; Chan, D. S.-H.; Leung, C.-H. Simple DNA-based logic gates responding to biomolecules and metal ions. *Chem. Sci.* **2013,** *4*, 3366-3380.

(11) Mondal, I.; Chattopadhyay, S. Development of multi-metallic complexes using metal-salen complexes as building blocks. *J. Coord. Chem.* **2019,** *72*, 3183-3209.

(12) de Ruiter, G.; van der Boom, M. E. Surface-confined assemblies and polymers for molecular logic. *Accounts of chemical research* **2011,** *44*, 563-573.

(13) Sha, Y.; Zhou, Z.; Hu, Y.; Zhang, H.; Li, X. Heterobimetallic polymers with pendant metallocenes: Correlating metallopolymer structures with properties. *Eur. Polym. J.* **2022,** *180*, 111579.

(14) Xue, K.; Hussain, S.; Fan, S.; Peng, X. Proton conducting metal–organic frameworks with light response for multistate logic gates. *RSC Adv.* **2023,** *13*, 12646-12653.

(15) Shu, F.; Chen, X.; Yu, Z.; Gao, P.; Liu, G. Metal–Organic Frameworks–Based Memristors: Materials, Devices, and Applications. *Molecules* **2022,** *27*, 8888.

(16) Zhou, J.; Huang, J. Photodetectors based on organic–inorganic hybrid lead halide perovskites. *Adv. Sci.* **2018,** *5*, 1700256.

(17) Liu, Y.; Li, F.; Chen, Z.; Guo, T.; Wu, C.; Kim, T. W. Resistive switching memory based on organic/inorganic hybrid perovskite materials. *Vacuum* **2016,** *130*, 109-112.

(18) Sarkar, M.; Chakraborty, R.; Taki, G. S.; Chakraborty, A. K. Design of basic logic gates using optical threshold logic. *ERX.* **2021,** *3*, 035021.

(19) Munakata, T.; Sinha, S.; Ditto, W. L. Chaos computing: implementation of fundamental logical gates by chaotic elements. *EEE Trans. Circuits Syst. I, Fundam. Theory Appl.* **2002,** *49*, 1629-1633.

(20) Budyka, M. Design principles and action of molecular logic gates. *Russian Chem. Bull.* **2014,** *63*, 1656-1665.

(21) Swarnakar, S.; Anguluri, S. P. K.; Sreevani, A.; Kumar, S. A novel structure of all-optical optimised NAND, NOR and XNOR logic gates employing a Y-shaped plasmonic waveguide for better performance and high-speed computations. *Opt Quantum Electron.* **2022,** *54*, 530.

(22) Anagha, E. G.; Jeyachitra, R. K. Review on all-optical logic gates: design techniques and classifications–heading toward high-speed optical integrated circuits. *Opt. Eng.* **2022,** *61*, 060902-060902.

(23) Brinkman, W. F.; Haggan, D. E.; Troutman, W. W. A history of the invention of the transistor and where it will lead us. *IEEE J. Solid-State Circuit* **1997,** *32*, 1858-1865.

(24) Magri, D. C. Logical sensing with fluorescent molecular logic gates based on photoinduced electron transfer. *Coord. Chem. Rev.* **2021,** *426*, 213598.

(25) Pan, Y.; Shi, Y.; Chen, Z.; Chen, J.; Hou, M.; Chen, Z.; Li, C.-W.; Yi, C. Design of multiple logic gates based on chemically triggered fluorescence switching of functionalized polyethylenimine. *ACS Appl. Mater. Interfaces* **2016,** *8*, 9472-9482.

(26) Stone, M. H. The theory of representation for Boolean algebras. *Trans. Am. Math. Soc.* **1936,** *40*, 37-111.

(27) Gaspar, D.; Martins, J.; Bahubalindruni, P.; Pereira, L.; Fortunato, E.; Martins, R. Planar dual-gate paper/oxide field effect transistors as universal logic gates. *Adv. Electron. Mater.* **2018,** *4*, 1800423.

(28) Wilkinson, R. H. A method of generating functions of several variables using analog diode logic. *IEEE Trans. Comput.* **1963,** 112-129.

(29) Easley, J. W. Transistor characteristics for direct-coupled transistor logic circuits. *IRE TEC.* **1958,** 6-16.

(30) Aharoni, H.; Likhterov, B. An alternative approach for the determination of the" OFF-ON" turnover process in four-layer semiconductor devices. *IEEE Trans. Educ.* **2000,** *43*, 434-438.

(31) Kahng, D. A historical perspective on the development of MOS transistors and related devices. *IEEE Trans. Electron Devices* **1976,** *23*, 655-657.

(32) Komatsu, H.; Matsumoto, S.; Tamaru, S.-i.; Kaneko, K.; Ikeda, M.; Hamachi, I. Supramolecular hydrogel exhibiting four basic logic gate functions to fine-tune substance release. *J. Am. Chem. Soc.* **2009,** *131*, 5580-5585.

(33) Jeon, Y.; Kim, S.; Seo, J.; Yoo, H. Contributions of Light to Novel Logic Concepts Using Optoelectronic Materials. *Small Methods* **2023**, 2300391.

(34) Lodha, A.; Singh, R. Prospects of manufacturing organic semiconductor-based integrated circuits. *IEEE Trans. Semicond. Manuf.* **2001,** *14*, 281-296.

(35) Lian, H.; Cheng, X.; Hao, H.; Han, J.; Lau, M.-T.; Li, Z.; Zhou, Z.; Dong, Q.; Wong, W.-Y. Metal-containing organic compounds for memory and data storage applications. *Chem. Soc. Rev.* **2022,** *51*, 1926-1982.

(36) Zhang, B.; Fan, F.; Xue, W.; Liu, G.; Fu, Y.; Zhuang, X.; Xu, X.-H.; Gu, J.; Li, R.-W.; Chen, Y. Redox gated polymer memristive processing memory unit. *Nat. Commun.* **2019,** *10*, 736.

(37) Yang, Y.; Wang, K.-Z.; Yan, D. Smart luminescent coordination polymers toward multimode logic gates: time-resolved, tribochromic and excitation-dependent fluorescence/phosphorescence emission. *ACS Appl. Mater. Interfaces* **2017,** *9*, 17399-17407.

(38) Lin, W.; Tan, Q.; Liang, H.; Zhang, K. Y.; Liu, S.; Jiang, R.; Hu, R.; Xu, W.; Zhao, Q.; Huang, W. Phosphorescence switch and logic gate of iridium (III) complexes containing a triarylboron moiety triggered by fluoride and an electric field. *J. Mater. Chem. C* **2015,** *3*, 1883-1887.

(39) Liu, X.-Y.; Han, X.; Zhang, L.-P.; Tung, C.-H.; Wu, L.-Z. Molecular logic circuit based on a multi-state mononuclear platinum (II) terpyridyl complex. *Phys. Chem. Chem. Phys.* **2010,** *12*, 13026-13033.

(40) Maurya, N.; Singh, A. K. Effective ensemble system for the identification of CN− based on a cobalt (ii) complex: a logic gate mimic. *New J. Chem.* **2017,** *41*, 4814-4819.

(41) Wang, Y.-W.; Liu, S.-B.; Yang, Y.-L.; Wang, P.-Z.; Zhang, A.-J.; Peng, Y. A terbium (III)-complex-based on–off fluorescent chemosensor for phosphate anions in aqueous solution and its application in molecular logic gates. *ACS Appl. Mater. Interfaces* **2015,** *7*, 4415-4422.

(42) Mondal, P. C.; Singh, V.; Jeyachandran, Y. L.; Zharnikov, M. Surface-confined heterometallic triads on the basis of terpyridyl complexes and design of molecular logic gates. *ACS Appl. Mater.* **2015,** *7*, 8677-8686.

(43) Cui, B. B.; Tang, J. H.; Yao, J.; Zhong, Y. W. A molecular platform for multistate near-infrared electrochromism and flip-flop, flip-flap-flop, and ternary memory. *Angew. Chem. Int. Ed.* **2015,** *54*, 9192-9197.

(44) Lin, G.; Lin, Y.; Cui, R.; Huang, H.; Guo, X.; Li, C.; Dong, J.; Guo, X.; Sun, B. An organic–inorganic hybrid perovskite logic gate for better computing. *J. Mater. Chem. C* **2015,** *3*, 10793-10798.

(45) Zhou, F.; Liu, Y.; Shen, X.; Wang, M.; Yuan, F.; Chai, Y. Low-voltage, optoelectronic CH3NH3PbI3− xClx memory with integrated sensing and logic operations. *Adv. Funct. Mater.* **2018,** *28*, 1800080.

(46) Kim, W.; Kim, H.; Yoo, T. J.; Lee, J. Y.; Jo, J. Y.; Lee, B. H.; Sasikala, A. A.; Jung, G. Y.; Pak, Y. Perovskite multifunctional logic gates via bipolar photoresponse of single photodetector. *Nat. Commun.* **2022,** *13*, 720.

(47) Dong, H.; Pang, S.; Zhang, Y.; Chen, D.; Zhu, W.; Xi, H.; Chang, J.; Zhang, J.; Zhang, C.; Hao, Y. Improving electron extraction ability and device stability of perovskite solar cells using a compatible PCBM/AZO electron transporting bilayer. *Nanomaterials* **2018,** *8*, 720.

(48) Noh, J. H.; Jeon, N. J.; Choi, Y. C.; Nazeeruddin, M. K.; Grätzel, M.; Seok, S. I. Nanostructured $TiO_2/CH_3NH_3PbI_3$ heterojunction solar cells employing spiro-OMeTAD/Co-complex as hole-transporting material. *J. Mater. Chem. A* **2013,** *1*, 11842-11847.

(49) Li, Z.; Chen, J.; Li, H.; Zhang, Q.; Chen, Z.; Zheng, X.; Fang, G.; Hao, Y. A facilely synthesized 'spiro'hole-transporting material based on spiro [3.3] heptane-2, 6-dispirofluorene for efficient planar perovskite solar cells. *RSC Adv.* **2017,** *7*, 41903-41908.

(50) Shu, F.; Chen, X.; Yu, Z.; Gao, P.; Liu, G. Metal–Organic Frameworks–Based Memristors: Materials, Devices, and Applications. *Molecules* **2022,** *27*, 8888.

(51) Liu, Y.; Wei, Y.; Liu, M.; Bai, Y.; Liu, G.; Wang, X.; Shang, S.; Gao, W.; Du, C.; Chen, J. Two-dimensional metal-organic framework film for realizing optoelectronic synaptic plasticity. *Angew. Chem. Int. Ed.* **2021,** *60*, 17440-17445.

(52) Magri, D. C. Logical sensing with fluorescent molecular logic gates based on photoinduced electron transfer. *Coord. Chem. Rev.* **2021,** *426*, 213598.

(53) Wang, X.; Kuang, J.; Wu, P.; Zong, Z.; Li, Z.; Wang, H.; Li, J.; Dai, P.; Zhang, K. Y.; Liu, S. Manipulating Electroluminochromism Behavior of Viologen-Substituted Iridium (III) Complexes through Ligand Engineering for Information Display and Encryption. *Adv. Mater.* **2022,** *34,* 2107013.

(54) Roztocki, K.; Bon, V.; Senkovska, I.; Matoga, D.; Kaskel, S., A Logic Gate Based on a Flexible Metal-Organic Framework (JUK‐8) for the Concomitant Detection of Hydrogen and Oxygen. *Chem. Eur. J.* **2022**, *28*, e202202255.

(55) Strauss, I.; Mundstock, A.; Treger, M.; Lange, K.; Hwang, S.; Chmelik, C.; Rusch, P.; Bigall, N. C.; Pichler, T.; Shiozawa, H. Metal–organic framework Co-MOF-74-based host–guest composites for resistive gas sensing. *ACS Appl. Mater. Interfaces* **2019,** *11*, 14175-14181.

(56) Li, B.; Zhao, D.; Wang, F.; Zhang, X.; Li, W.; Fan, L. Recent advances in molecular logic gate chemosensors based on luminescent metal organic frameworks. *Dalton Trans.* **2021,** *50*, 14967-14977.

(57) Kaniewska, K.; Bollella, P.; Katz, E., Implication and Inhibition Boolean Logic Gates Mimicked with Enzyme Reactions. *Chemphyschem.* **2020,** *21*, 2150-2154.

(58) Zhang, J.; Fu, H.; Chu, X. Metal–Organic Framework Nanoparticles Power DNAzyme Logic Circuits for Aberrant MicroRNA Imaging. *Anal. Chem.* **2021,** *93*, 14675-14684.

(59) Dalapati, R.; Biswas, S., Aqueous phase sensing of Fe^{3+} and ascorbic acid by a metal–organic framework and its implication in the construction of multiple logic gates. Chem. Asian J **2019**, *14*, 2822-2830.

(60) Bi, H.; Duarte, C. M.; Brito, M.; Vilas-Boas, V.; Cardoso, S.; Freitas, P. Performance enhanced UV/vis spectroscopic microfluidic sensor for ascorbic acid quantification in human blood. *Biosens. Bioelectron.* **2016,** *85*, 568-572.

(61) Sun, T.; Wang, P.; Fan, R.; Chen, W.; Hao, S.; Yang, Y. Functional microscale single-phase white emission lanthanide MOF for tunable fluorescent sensing and water quality monitoring. *J. Mater. Chem. C* **2019,** *7*, 3598-3606.

(62) Zhang, Y.; Yan, B. A point-of-care diagnostics logic detector based on glucose oxidase immobilized lanthanide functionalized metal–organic frameworks. *Nanoscale* **2019,** *11*, 22946-22953.

(63) Halliwell, B.; Chirico, S. Lipid peroxidation: its mechanism, measurement, and significance. *Am. J. Clin. Nutr.* **1993,** *57*, 715S-725S.

(64) Kang, J.; Huo, F.; Zhang, Y.; Chao, J.; Strongin, R. M.; Yin, C. Detecting intracellular ClO-with ratiometric fluorescent signal and its application in vivo. *Sens. Actuators B Chem.* **2018,** *273*, 1532-1538.

(65) Zou, C.; Foda, M. F.; Tan, X.; Shao, K.; Wu, L.; Lu, Z.; Bahlol, H. S.; Han, H. Carbon-dot and quantum-dot-coated dual-emission core–satellite silica nanoparticles for ratiometric intracellular Cu^{2+} imaging. *Anal. Chem.* **2016,** *88*, 7395-7403.

(66) Gong, M.; Liao, C.; Yang, J.; Kang, F.; Gu, J. Smart logic gates constructed by fluorescent-customizable nanoMOFs for diseases monitoring. *Appl. Mater. Today* **2020,** *20*, 100760.